A neutronics optimization approach for preliminary design and safety of nuclear reactors for nuclear thermal propulsion

A neutronics optimization approach for preliminary design and safety of nuclear reactors for nuclear thermal propulsion

Samuele Meschini[a,*], Antonio Cammi[b]

[a]*Politecnico di Torino, Department of Energy, Corso Duca degli Abruzzi 24, 10129, Torino, Italy*

[b]*Politecnico di Milano, Department of Energy, CeSNEF-Nuclear Engineering Division, Via Ponzio 34/3, 20133, Milano, Italy*

Abstract

Nuclear thermal propulsion is a key technology for long-range spaceflight, as demonstrated by the rising interest from space agencies, especially NASA. A preliminary design involves the exploration of many reactor configurations, until a configuration that meets all the design requirements is found. Trade-offs among different design fields, such as neutronics, thermal-hydraulics, safety and rocket performances are unavoidable. Design engineers have to run a large amount of simulations because of the multitude of possible reactor configurations and the different analyses that must be carried out. The present work investigates an optimization approach for the design of a LEU reactor with CERMET fuel, to find a configuration that fulfils neutronics, safety and NASA requirements for a nuclear thermal rocket. A neutronics analysis constitutes the basis of the work, but accidental scenarios and thermal-hydraulics analysis are performed as well, to assess reactor safety and rocket performances. The optimization procedure simulates different configurations and gradually reduces the design space to be explored, until an optimal region is found. In this way, unnecessary simulations are avoided. A Python script is developed to handle the whole analysis, from pre-processing to post-processing, including the integration between the neutronic code Serpent and MATLAB®. Once the optimal region is found, the most promising configurations are identified by comparing different performance metrics retrieved from the neutronics analysis. A safety analysis that simulates the reactor behaviour in four accidental scenarios is carried out on this smaller group of reactor configurations. Finally, reactors that fulfil safety requirements undergo a thermal-hydraulic analysis, which verifies that thermal limits are not exceeded and evaluates rocket performances. The approach successfully reduces the number of configurations to explore, and limits additional analyses to those configurations that are truly competitive. Furthermore, configurations in the optimal region achieve better performance than the initial configuration. It is also found that the most demanding constraints relate to safety: many promising configurations were discarded because they cannot meet safety criteria. This highlights the necessity of including safety analyses in the initial phase of reactor designs. It is concluded that a LEU, CERMET-fuelled reactor design can be considered challenging but feasible, and the approach presented in the work may be applied to find an optimal configuration for a preliminary reactor design.

Keywords: Nuclear Thermal Propulsion (NTP), CERMET, Low-Enriched Uranium (LEU), Serpent 2, Neutronics optimization, Submersion accidents.

*Corresponding author. Email: samuele.meschini@polito.it

1. Introduction

In the last years, new interest in nuclear space propulsion has been shown by space agencies. The next big step in space exploration will probably be bringing a man to Mars. Progresses have been made in the on-site power generation, thanks to the stationary reactor design Kilopower [1], but the Earth-Mars travel is still an open field of research. Such a long journey poses many challenges that are still not completely overcame: energy must be provided to the spacecraft, reliability and safety must be assured for the whole mission time and, finally, the cost should be kept below reasonable limits. The most promising technology able to fulfil these requirements on a short-time term is Nuclear Thermal Propulsion (NTP). Indeed, NASA defines NTP as a key technology for long-range spaceflights [2], [3].

The design of a space reactor is a complex problem, constituting a harsh challenge in terms of modeling, procedures and resources. Most of the works on this topic focus on a single area, which may be neutronics, thermal-hydraulics or safety. The deep level of detail of such studies makes the outcome extremely valuable for NTP advancement; however, different approaches can be investigated. Few explicit, general methodologies have been presented to deal with a space reactor design and optimization. SPOC (Space Propulsion Optimization Code) is focused on all the neutronics and thermal-hydraulic aspects of space reactor design [4]. A more case-related code (ATHENA) has been developed for the SP-100 space reactor, allowing thermal-hydraulics and accidental scenarios analyses [5]. Despite being developed for terrestrial applications, ARMI® (Advanced Reactor Modeling Interface) philosophy is highly instructive [6]. All those codes, and the underlying approaches, recognize the importance of cross-field analyses and the necessity to explore different design options. When the design process is faced in its completeness, the analyst is forced to adopt an iterative procedure, which may be greatly time consuming and leads to drastic modification of the initial design. Classical coupled approach between neutronics and thermal-hydraulics partially tackle the problem, but the major constraints come from safety. Thus, before starting time consuming simulations, a more explorative-oriented approach should be adopted. In doing so, a global view of the system is retrieved. Furthermore, if a preliminary huge effort is done in the development of a general procedure, subsequent analysis will be drastically eased. This allows the designer to focus more on engineering issues and less on the development of an ad-hoc model for the specific case. Automation and scalability are key concepts for the diffusion and the improvement of an essential technology like nuclear space propulsion.

Starting from Rover and Nerva projects, many different reactor configurations have been designed and tested along the years. A detailed and comprehensive review on fuel and fuel elements tested at the Los Alamos Scientific Laboratory up to the seventies can be found in [7]. In the first decades of research in this field, composite fuels were heavily investigated as the most promising solution. At the present time, the focus has been shifted towards CERMET (CERamic-METallic) [3], Carbide and even more advanced fuels. The reader can found a detailed review on fuels for Low Enriched Uranium (LEU) space reactors in [8]; more advanced fuels, such as tri-carbides, have been investigated too [9]. CERMET fuels show better thermo-mechanical properties and improved chemical compatibility with hydrogen if compared to composite fuels. Specifically, W-matrix CERMET fuels are the most suitable to address the main issues encountered in Rover and Nerva program. Carbide fuels allow for the highest operational temperature in the reactor. The brittle nature and the low uranium solubility at high temperature are the main issues related to these fuels. Fuels are not limited to the solid state, being liquid and gaseous core studied as well [10], [11]. However, solid core remains the most feasible option with the available technologies [11], thanks to the experience accumulated during past programs. Uranium is by far the most common fuel for NTP, with U-235 enrichment above 90%: High Enriched Uranium (HEU) design have many advantages with respect to LEU design, related the exploitation of a fast spectrum core [12]. HEU fuels allow to reach extremely high performance with modest reactor size [13], a desirable feature for space reactors. Many studies have been conducted in the neutronics and thermal-hydraulics fields , showing the possibility to reach specific impulses as high as 900 seconds with a

consistent thrust (110 kN) [3], [14]. Recently, LEU reactors have gained popularity, thanks to their inherent proliferation resistance. The lower fissile mass present in a LEU reactor must be balance by an increase in fission probability: this can be achieved by softening the neutron spectrum down to thermal energies. The benefits related to LEU fuel may overcome the additional efforts in designing a thermal spectrum reactor, namely the need of moderator elements and the minimization of neutron parasitic absorptions. A detailed analysis on LEU reactors for NTP can be found in [15] and subsequent works [16], which demonstrate the feasibility and the competitiveness of a LEU design. Safety studies are more limited, even if extremely important: due to the radiological hazard, a space reactor must be able to withstand a possible accident without becoming supercritical. A specific class of accidents, namely submersion accidents, are considered in safety studies for both HEU reactors [17], [18] and LEU reactors [19], [20]. Those include reactor submersion in different materials, such as dry sand, wet sand and water. Safety systems range from Spectral Shift Absorbers (SSA) addition in the core to active systems like control rods and Control Drums (CD). When considering also reactor safety, the neutronics design must address two competing requirements [21]: on one hand, the excess reactivity must be large enough to allow reactor operations during the expected mission time; on the other hand, the reactor must reach subcriticality following a submersion accident.

The present work focuses on the development of a systematic analysis to quickly explore different reactor configurations, to find an optimal solution which satisfies neutronics, thermal-hydraulics and safety requirements. Even though realistic and consistent results are sought, the goal of the work is not to provide design parameters, but to propose and investigate an alternative design procedure. The core of this analysis is the neutronics optimization, with a safety-oriented approach. To do so, a parametric analysis on the main design parameters has been implemented, which exploits a tight coupling between the neutronic code Serpent [22] and MATLAB®. The whole procedure, from the pre-processing to the post-processing, has been automated through a Python script that integrates Serpent and MATLAB®. User induced errors and bias on the model are completely removed, the analyst is freed from the burden of building a new model for each configuration and the time between subsequent simulations is minimized. The metric defined to compare different configurations relies on performance parameters taken from neutronics, thermal-hydraulics and rockets science. Specifically, excess reactivity, reactivity control worth, shutdown margin and maximum fuel temperature are considered from the neutronic and safety viewpoint, whereas outlet coolant temperature, mass flow rate and reactor mass define the system performances. This allows for a strong reduction of computational time, limiting the simulations to the configurations which may be truly competitive. The lightness of this approach and its extreme flexibility are key features of the whole analysis.

The structure of the paper is the following: in Section 2 the space reactor model is introduced. Section 3 describes the methodology for the neutronics, thermal-hydraulics and safety analysis, and the optimization procedure that is applied. Section 4 presents the results of the analysis. In Section 5 a discussion on the optimization approach is proposed, in light of the results obtained by the simulations. Section 6 draws the conclusions.

2. Reactor model

In this section, the reactor model is presented. The starting configuration is a derivation of the NERVA design [15], [16]**.** The reactor features hexagonal, solid fuel and moderator elements arranged in a cylindrical core, surrounded by a graphite sleeve (Figure 1 and Figure 2). The core is a cylinder of 35 cm radius and 75 cm height, with two radial enrichment zones. A radial and an axial reflector are also present. The radial reflector has 12 cylindrical holes to host an equal number of control drums. Both radial and axial reflector are 20 cm thick: the axial reflector is present only on the upper core region, being the condition on the lower region extremely harsh for the reflector materials. Indeed, the high-temperature propellant is gathered in the lower plenum and sent to the nozzle. None of the materials commonly used for a reflector can sustain such high temperatures in the lower core region. The enrichment zones are respectively 17% and 20% enriched in U-235. The coolant, which works also as propellant, is hydrogen. To provide the required specific impulse and thrust, the reactor power is set at 450 MW. Additional data on the reactor model is provided in the Appendix.

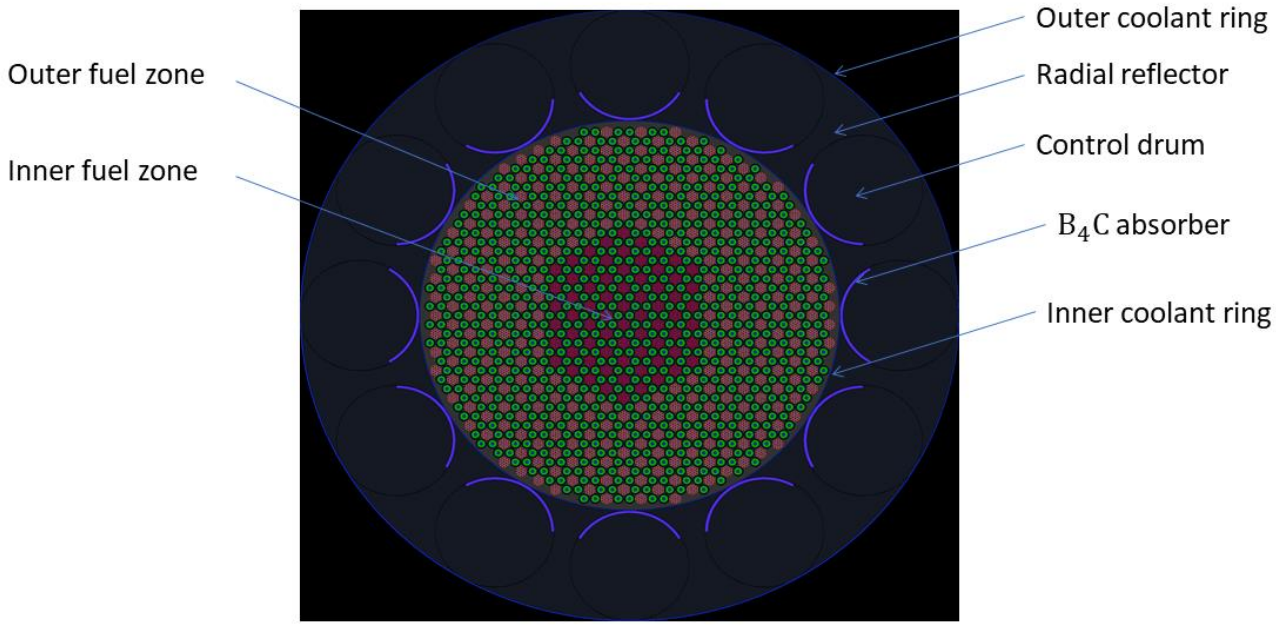

Figure 1 - Poloidal cross section of the reactor core, at midplane. The main components are depicted.

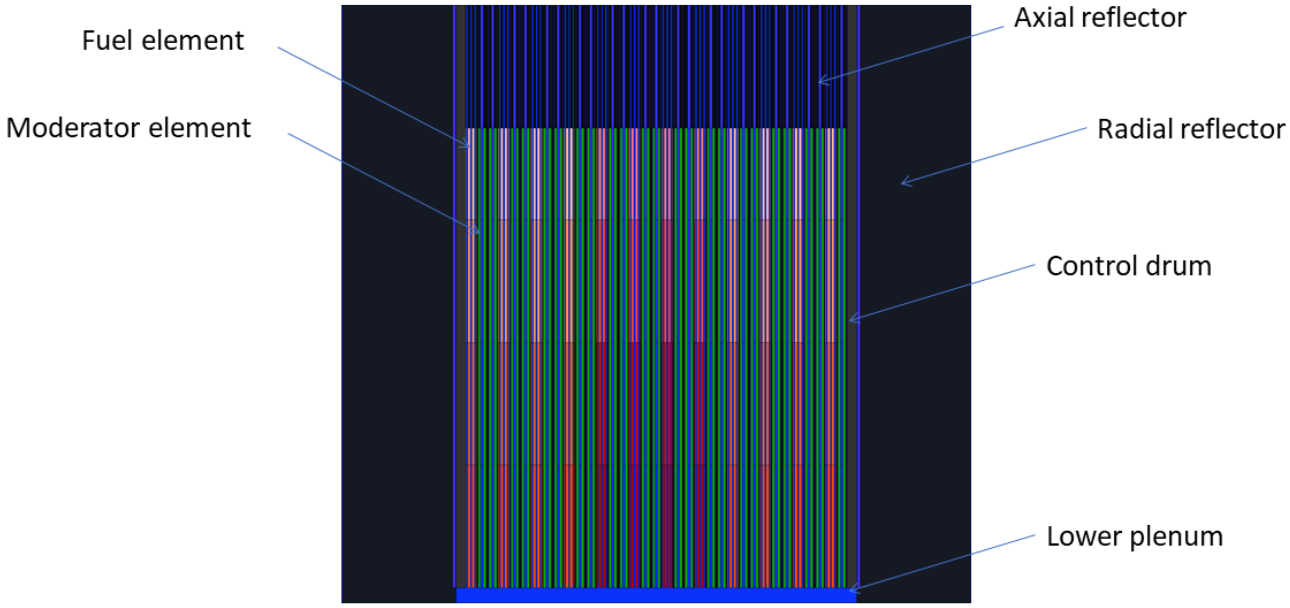

Figure 2 - Axial cross section of the reactor core. The main components are depicted.

2.1 Fuel elements

Fuel elements (Figure 3) have a hexagonal shape and are packed with the moderator elements. The ratio of fuel elements to moderator elements is 1:2. The flat-to-flat distance is 1.905 cm. Each fuel element is crossed by 19 coolant channels with a radius of 0.1397 cm. Two different fuel materials have been selected for the present work: a composite fuel and a CERMET fuel.

Composite fuels have been extensively studied in the past decades during Rover and Nerva programs [7]**.** The most performing fuel was found to be $(\mathrm{U,Zr})\mathrm{C}$ with a graphite matrix. Zr addition to the fuel significantly increases the melting temperature, and the graphite has a low absorption cross section. However, this fuel is not exempt of weak points: the graphite matrix reacts with the high temperature coolant, leading to a fast erosion. To overcome this issue, a ZrC or NbC coating was implemented in the coolant channels. ZrC has better neutronics properties (low absorption cross section), but its melting temperature is lower than NbC melting temperature, at least for standard production techniques [23]. Novel techniques claims to be able to raise ZrC melting temperature up to 3900 K [8]**.** In the present work, NbC is chosen as coating for the composite fuel.

CERMET fuels are made of $\mathrm{UO_2}$ or UC and a refractory material. Many refractory materials were tested for space applications, such as $\mathrm{Ir, Nb, Ta, Re, Mo, W}$ [8]**.** Their inclusion in the fuel matrix greatly increase fuel melting temperature, providing reasonable thermal conductivity and mechanical strength. Since the system under study is a LEU reactor, these materials should have low absorption cross section and good chemical compatibility: these two limiting factors lead to the choice of tungsten-based fuels. To lower the absorption cross section, high enrichment in $\mathrm{W\text{-}184}$ is required. The CERMET considered in this work is $\mathrm{UO_2}$-$\mathrm{ThO_2}$-W, with tungsten 99 at% enriched in its low-absorption isotope $\mathrm{W\text{-}184}$. CERMET fuel elements feature a $\mathrm{W\text{-}Re}$ coating in the coolant channels.

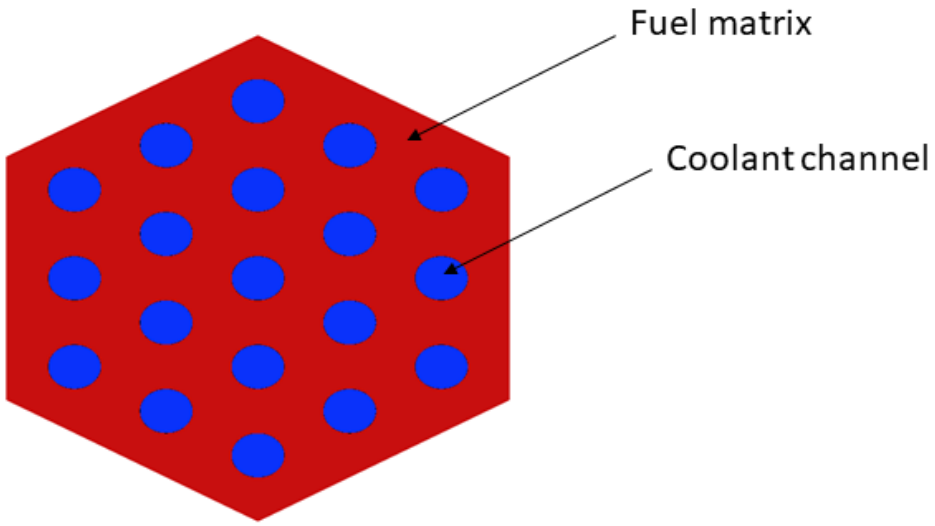

Figure 3 - Hexagonal fuel element. The fuel matrix is in red, the 19 coolant channels in blue.

2.2 Moderator elements

The choice of moderator element materials is limited to solid, because of volume constraints. The most promising materials are graphite, beryllium, zirconium hydrate ($ZrH_{1.8}$) and lithium hydrate (^{7}LiH). The first two materials have high melting temperature, making them particularly suitable for this class of reactor. However, beryllium suffers from loss of structural integrity due to He production, while graphite reacts with the high temperature hydrogen. ^{6}Li in Li, even if limited, has a high absorption cross section, leading to helium and tritium production. Thus, for compatibility issues, $ZrH_{1.8}$ is the most suitable moderator, even though its thermo-mechanical properties are not comparable to those of graphite and beryllium, and its moderating capability is lower than ^{7}LiH.

Moderator element structure (Figure 4) is designed to prevent $ZrH_{1.8}$ to reach high temperatures. Starting from the inner coolant channel, a Zircaloy cladding protects the moderator; an annular coolant channel surrounds the moderator itself, while an insulator in ZrC encapsulates the whole structure, isolating the moderator from the neighbour fuel elements. Finally, a graphite body gives the hexagonal shape to the element.

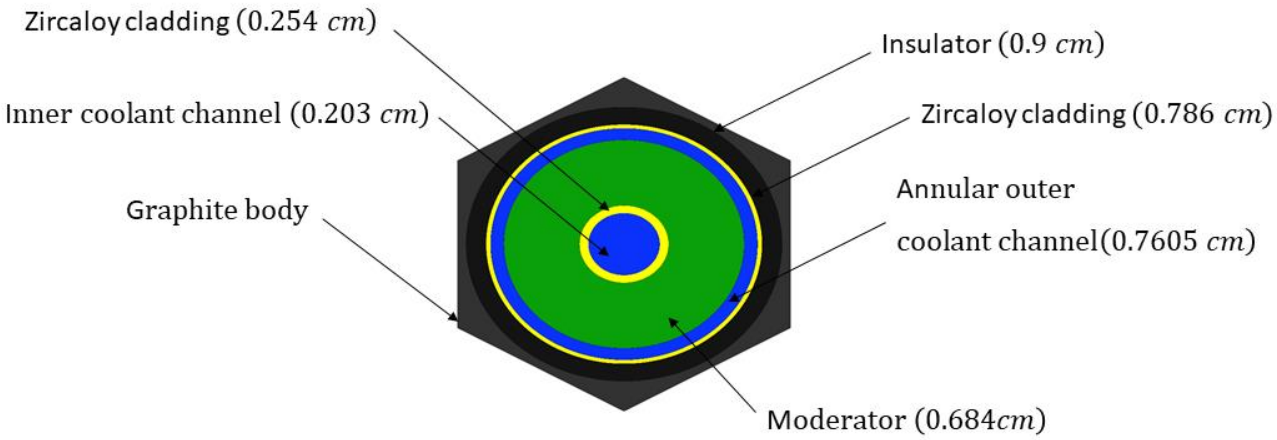

Figure 4 – Hexagonal moderator element. The outer radius of each cylindrical component is reported in bracket. The colour legend is the following: Graphite body (grey), thermal insulator (black), Zircaloy (yellow), moderator (green), coolant (blue).

2.3 Reflector and control drums

In space propulsion reactors, the reflector is extremely important not only for the neutron leakage decrease that it provides, but also for its active reactivity control. Furthermore, the reflector mass gives a large contribution to the total reactor mass, making it a component of interest when dealing with mass reduction optimization. The radial reflector is made of metallic beryllium, which combines acceptable density (1.85 g/cm^3) with good reflective and moderating properties. It surrounds the core for the entire length, and it is equipped with 12 rotating control drums, made of metallic Be, with a 120° circular sector of B_4C absorber. CD working principle is simple: when the absorber is facing the core, the neutron absorption is maximum, allowing to bring the reactor in a subcritical state; when the absorber is facing outward, the positive reactivity insertion is maximum. Tuning the rotational angle keeps the reactor critical. CD control worth should be high enough to compensate reactivity losses due to burnup and to bring the reactor subcritical even in accidental scenarios. Many different control systems have been proposed in the past: control shutter, slats, or petals layout [24] and control rods. Nevertheless, control drums are the most endorsed technology, thanks to their easily implementation and to their widespread adoption in previous design. For these reasons, control drums are chosen as reactivity control system in this work.

The axial reflector is crossed by the totality of the coolant channels (Figure 2), and it is located only on the top of the core, being the temperature around the core bottom too high for both Be metal and BeO. Metallic beryllium is not suitable for the upper axial reflector either, because at temperatures $T > 600$ K it is prone to interact with the hydrogen flowing in coolant channels [12]. The problem is overcame using BeO instead of Be.

3. Methodology

Many previous works focused only on a specific design area, such as neutronics or thermal-hydraulics. The accidental scenarios analysis is usually tackled as a standalone problem and not as an issue that leads the design. Trying to overcome these limitations, the present work approaches the design in a more complete way, investigating various configurations until a reactor design that is safe, highly performing and that fulfils

NASA requirements [25] is found. First, a composite fuelled reactor model is built, according to the description provided in Section 2. Results from the simulation are compared with the C-LEU-NTR ([15], [16]) design, in order to verify the model. Then, the composite fuel is replaced by the CERMET fuel, and the optimization of this configuration is carried out. The neutronic code chosen in this work is Serpent [22]. The nuclear data library used for Serpent simulations is JEFF 3.1 [26]. A strong effort was made to elaborate a code which eliminates user's intervention and errors, minimizes time between simulations and handles all the simulation phases integrating different software (Serpent and MATLAB®). Optimizing the computational capabilities translates in a huge number of configurations that must be compared: to do so efficiently, performance metrics from the neutronics, thermal-hydraulics and rocket science have been selected. These quantities should synthetize the features, performance and issues of the reactor, avoiding additional, expensive simulations. The performance metrics chosen are: k_{eff} (both in nominal and failure conditions), hot channel factor, reactor mass and fissile mass. The exploration and optimization procedure is performed by varying geometry and layout, testing different materials (except for fuel and moderator), changing the number of enrichment zones and enrichment value itself. The optimization goals on which this work focuses are:

- reactivity optimization and safety features strengthening;
- minimization of fissile material and excess reactivity;
- peaking factors reduction and reactor performances maximization;
- reactor mass reduction.

The strong interconnection between different design areas are evident: the variation of any of the previous quantities inevitably affects the others. The main issues faced by a LEU reactor are summarized to better explain this point. First, the excess reactivity should be high enough to ensure criticality for the whole mission time, but reasonably low to avoid supercriticality in accidental scenarios. Second, CD are the only active control system: this means that the CD reactivity worth must be known for every possible angle of rotation, and the CD absorber thickness needs to be tuned to find the optimal value of control worth. Furthermore, the reflector thickness has a dramatical impact on both safety and performance, being also the heaviest component and strongly affecting neutron flux distribution. Finally, peaking factors must be evaluated and kept as low as possible, since any hotspot would raise safety concerns and reduce the overall reactor performances. In a system where the mass is a primary constraint, and refuelling is not possible, finding a configuration that can deal with all the previous issues requires a systematic approach. The procedure can be visualized in the flowgraph reported in Figure 5. Operatively speaking, the whole process can be schematized as in Figure 6.

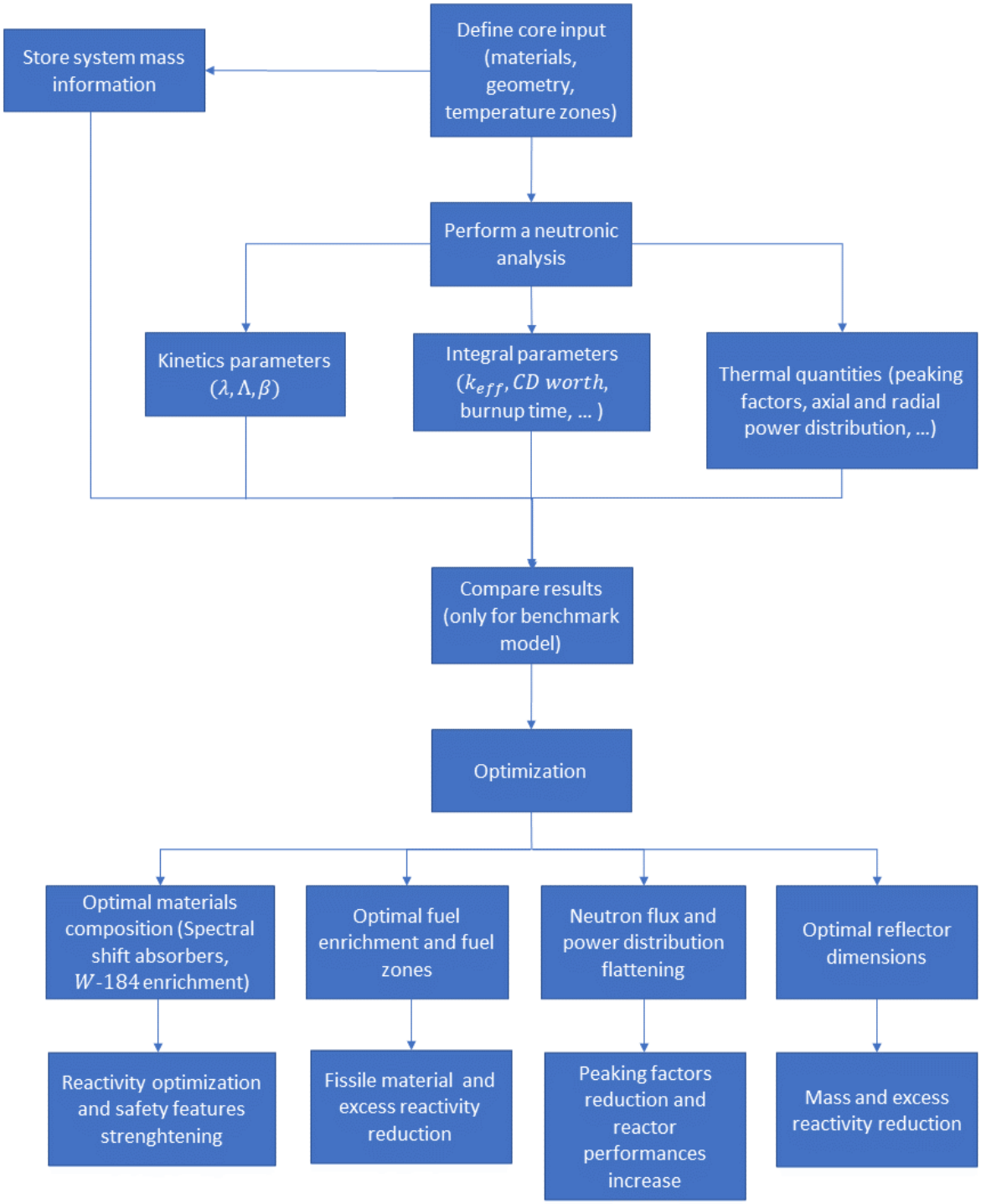

Figure 5 – Flowgraph describing the general procedure followed in this work.

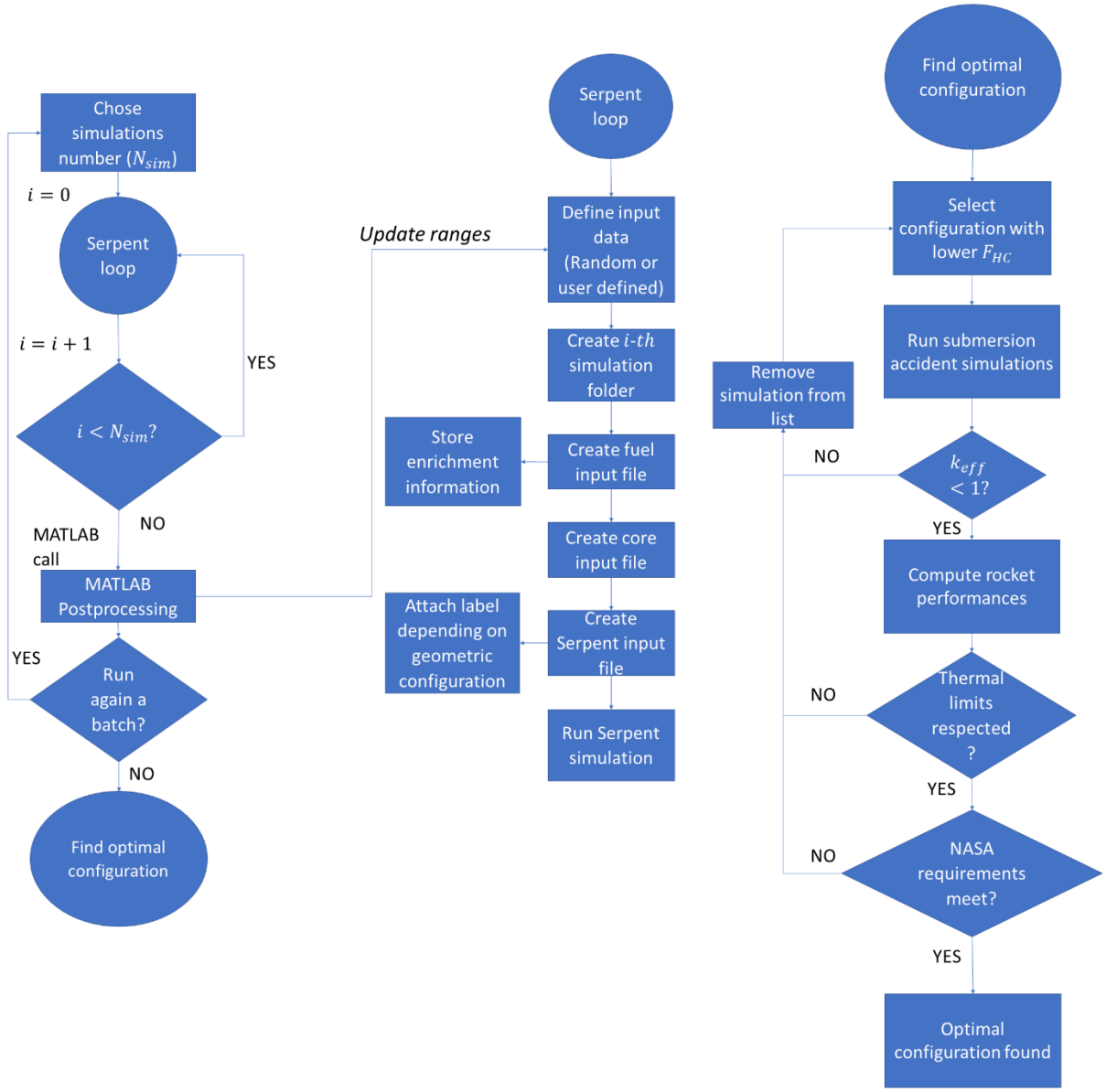

Figure 6 - Operative flowgraph for the simulation process and post-processing

The only input required for the Python script handling the simulations is the number of simulations itself, N_{sim}. Then, starting from a template input file, the script modifies the reactor parameters of interest, changing them randomly in ranges previously defined by the user in a separate file. By default, the script explores different enrichment and enrichment zones. The post-processing performed by MATLAB® has two main functions. First, it extracts the main quantities used for the comparison and updates (reduces) the possible ranges of input parameters. Second, it detects the most promising configuration. The first function goal is to gradually reduce the possible design space, by removing those parameters values that do not optimize the reactor configuration. This is done by filtering the simulations through a series of hierarchical constraints. The hierarchy of constraints is defined by the user. If a specific parameter value is found in simulations that are discarded, and does not appear frequently in the simulations that satisfy a certain constraint, the value is considered not optimal and removed from the possible input values. The pseudocode describing this process can be found in the Appendix. The strongest constraint applies on the k_{eff}, a second constraint deals with the hot channel factor and the last constraint removes configurations with unnecessary

additional mass. Batches of 100 simulations are run to provide a suitable number of outputs to reduce the design space. Nine batches of 100 simulations were run to reduce the design space. A final batch of 50 simulations was run to identify the most promising configuration. Because of safety requirements, the most promising configuration was identified as the one which minimizes the hot channel factor and excess reactivity. Indeed, explicitly addressing criticality in design and safety criteria is one of the recommendations from the recent NASA technical report [27]. Fissile and total mass saving have been considered secondary parameters for the choice, not directly influencing the reactor safety. Finally, different safety systems were tested on the best configuration, to find the most suitable for this reactor class.

3.1 Neutronics analysis

A neutronic analysis is the starting point for reactor design. It returns crucial information on core criticality, fuel depletion, neutron flux, power distribution, control system reactivity worth and dynamics parameters. All those parameters heavily affect reactor behaviour and the optimal set of parameters that meet all the requirements should be found. If the excess reactivity is too low, the reactor cannot operate for the required mission time; conversely, if it is too large, supercriticality issues arise in accidental scenarios, suggesting an optimization focused on fuel enrichment and layout. The neutron flux and the consequent power distribution highlight possible optimizations from the thermal viewpoint, which can be performed acting on fuel enrichment, fuel enrichment zones, reflector design and core thermal-hydraulics. Since the reactor will operate in space without any human intervention, the control system must handle any possible scenario: this implies that the CD reactivity worth must be known and tuned precisely.

The Monte Carlo-based code Serpent is chosen for the simulations. Temperatures variations inside the core were accounted through a division in four constant-temperature zones (see Appendix for additional details). The thermodynamics properties for the various materials in the core were recovered from [7], [28], [29]. The temperature assigned at each zone is the mean between its upper and lower boundary, assuming the same temperature profile of the SNRE [16]**.** Once the model has been verified by comparing the composite fuel configuration with the results from C-LEU-NTR ([15], [16]), the CERMET fuelled configuration is analysed and optimized.

3.2 Safety analysis

An accidental scenarios analysis is mandatory when designing a nuclear reactor. Safety must be ensured in any possible reactor operation and failure scenario, maintaining k_{eff} below criticality. There are many concerns related to nuclear reactors for space applications, due to possible failures in the first mission stage, when the rocket is escaping Earth gravity. Those go under the name of submersion accidents: following a launch abort scenario, the reactor falls back to the Earth, where it is submerged by different materials. This situation is extremely dangerous for both population and environment. The reactor may reach supercriticality, increasing its power exponentially until the core melts, with a consequent release of radioactivity. Among these scenarios, submersion in dry sand, submersion in wet sand, submersion in seawater and submersion in seawater followed by reflector dismantling are the most relevant. In those scenarios the reactor temperature is brought below room temperature, an infinite reflective medium surrounds the core and a moderating material fills the channels, with a consequent large burst of positive reactivity. CD must be designed properly to provide enough shutdown margin. However, if the reflector gets dismantled, the reactor loses its active control component. In this situation, the core may rely on its passive reactivity control system only. Indeed, even if design implementing control rods have been proposed [20], it

is preferable to avoid such safety systems, due to unavoidable increase of system complexity and reliability related issues. In the present work, SSA addition, control rods and an advanced control drum system are investigated. The spectral shift absorbers that have been tested are: Eu_2O_3, Gd_2O_3, Ir, Re, Sm_2O_3. Both natural and high-absorbing isotopes were considered. Only one SSA at a time was tested.

3.3 Thermal-hydraulics analysis

Thermal-hydraulics analysis is the last step for a preliminary design. The main goals of this analysis are to check whether thermal limits are not exceeded in any core element and to evaluate (or increase, if possible) the overall rocket performances. The first objective is mandatory for safety reason: if the temperature raises up to materials melting point, local melting occurs. This is an extremely dangerous situation because the whole reactor may be compromised, and radioactive elements may escape the core. Furthermore, ensuring that the temperature remains below safety limits, at least for nominal operations, has a direct impact on propulsion performances. A useful parameter to monitor thermal limits is the hot channel factor, defined as the ratio between the power production in the hottest element and the power production in the average fuel element. For large values of the hot channel factor F_{HC}, the high temperatures along the hot channel limit the average outlet coolant temperature, bounding both the specific impulse and the thrust. A thermal-hydraulics analysis may be carried out by a CFD software that return almost any attainable quantity of interest, with a complete view of both fluid dynamics and heat exchange process. However, this approach does not fit with the philosophy of the present work, which aims to develop a model for space reactor design that is light, applicable even with limited computational resources and easily integrable with other codes. In this perspective, the fuel elements cannot be analysed as they are, because of their geometry complexity (Figure 3). It is assumed that each cooling channel is surrounded by a cylindrical section of fuel. The equivalent outer radius (Figure 7) of the fuel is computed so that the mass surrounding each channel is 1/19 of the total fuel element mass. Radial symmetry is assumed. Axial conduction is neglected, and the outer fuel surface is assumed adiabatic. The thermal conductivity of the coating is assumed constant due to its small thickness. Finally, the system is considered in steady state.

Before entering the fuel channels, the coolant follows two different paths: a fraction of the coolant is sent to the moderator elements and then to the upper plenum, whereas the remaining coolant fraction is sent directly to the upper plenum. In the upper plenum the two flows are mixed, and then sent to the fuel elements. In this way the average coolant temperature at the fuel element inlet is lower than the outlet coolant temperature from the moderator element. Thus, additional cooling can be provided to the fuel elements.

The inlet coolant temperature in the upper plenum is set at 125 K. The outlet coolant temperature from the moderator elements is computed as:

$$T_{c,out,mod} = \frac{P_{mod}}{\dot{m}_{mod} \cdot \bar{c_p}} + T_{c,in,mod}$$

where P_{mod} is the power deposition inside the moderator elements, $\dot{m}_{mod}$ is the coolant mass flow rate in the moderator elements, $\bar{c_p}$ is the average coolant specific heat and $T_{c,in,mod}$ is the inlet coolant temperature in the moderator elements. The fuel inlet coolant temperature is therefore computed as:

$$T_{c,in,fuel} = \frac{\dot{m}_{mod}\, T_{c,out,mod} + \dot{m}_{pl}\, T_{inlet}}{\dot{m}_{mod} + \dot{m}_{pl}}$$

where $\dot{m}_{pl}$ is the coolant mass flow rate that is directly sent to the upper plenum and T_{inlet} is the reactor inlet coolant temperature. The total mass flow rate, $\dot{m}_{tot} = \dot{m}_{mod} + \dot{m}_{pl}$, is initially assumed equal to 12.5 kg/s. $\dot{m}_{mod}$ has been computed iteratively until the moderator outlet coolant temperature was low enough to avoid damages to the moderator elements. For $\dot{m}_{mod} = 4.5\ \mathrm{kg/s}$ the moderator outlet coolant temperature is kept below 840 K.

To identify the hot channel, the *set cpd* card was added to Serpent input. *set cpd* returns the core power distribution at different levels, including fuel element level. In that way, it is possible to quantify the power deposition in the average element and in the most heated element; also, the hot channel factor can be computed. Still, the axial power profile is not known. One approach consists in placing a Serpent detector in the hottest element, and run again the simulation. This is clearly not applicable if many simulations must be run, because it doubles the number of simulations required. Instead, a simpler approach is chosen. A detector is placed on a generic fuel element located at half the core radius. This element is considered representative of the average coolant channel. The axial power profile is then reconstructed from the detector output. If the total power deposited in this fuel element does not match the average power computed by the *set cpd*, the power profile is scaled accordingly. The same procedure is applied in the hot channel, where the scaling is performed according to the hot channel factor.

Once the average channel and the hot channel profiles are defined, the fuel, coating and coolant temperature are evaluated by dividing the fuel element in n axial bins. At each bin, the coolant temperature is computed from an energy balance. The heat transfer coefficient between coolant and coating has been evaluated by means of the Dittus-Boelter correlation. Then, the coating temperature and the fuel temperature are evaluated through the thermal resistance method, namely by iteratively solving the equation:

$$q' = R_{th,i}\Delta T_i$$

where q' is the power per unit length in the j-th bin, $R_{th,i}$ and ΔT_i are the thermal resistance and the temperature difference of material i, in that case the W-Re coating and the CERMET fuel in the j-th bin.

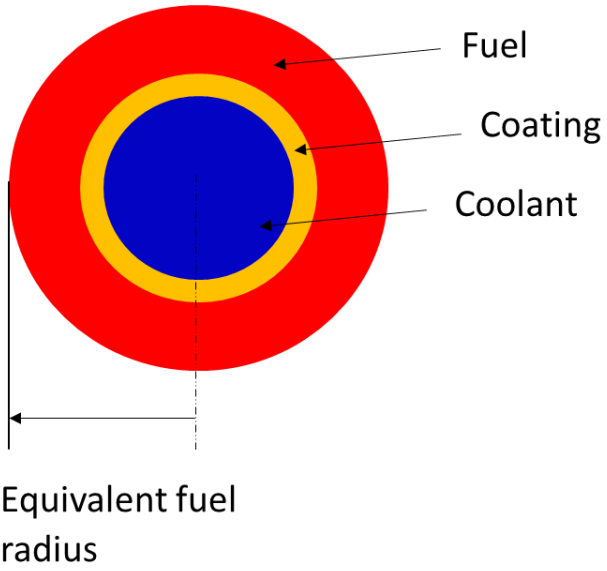

Figure 7 - Geometrical representation of a coolant channel surrounded by fuel. The equivalent radius of the fuel is depicted. The coating thickness is not in scale.

4. Results

4.1 Model verification

Once the base configuration has been set, a preliminary analysis was performed to check the model validity. Table 1 shows a comparison of the main neutronics quantities between the reference configuration and the present model.

Table 1 - Model verification. Comparison between C-LEU-NTR [16] *and the composite fuelled reactor.*

	C-LEU-NTR [16]	**Current model**	**Relative difference**
k_{eff} [-]	1.11610	1.12744	1.0%
β_{eff} [-]	0.00717	0.00713	0.5%
Λ [μs]	106	109	2%
Reactor mass (no shielding) [kg]	2016	2054	1.8%

Recalling that two different software were used for these two models (MCNP5 for the C-LEU-NTR, while Serpent for the present work), and that the way in which temperature effects may be taken into account is not unique (e.g., more temperatures zone can be defined), the differences look acceptable. The reasons behind the choice of the quantities in Table 1 is readily explained: k_{eff} is an integral value which can be considered representative of the whole neutronics phenomena in the core; the effective delayed neutron fraction β_{eff} and the mean generation time Λ are related to neutrons kinetics and reactor dynamics, thus affecting control and safety; reactor mass is a target parameter to be minimized from the propulsion viewpoint. According to the comparison, the model is considered correct, and an in-dept analysis on the CERMET fuelled rector can be performed.

4.2 CERMET base configuration

A complete analysis following the approach described in the previous section allows to gather an extremely large amount of data which is presented in this sub-section. A sensitivity analysis on three nuclear data libraries has been performed prior to any simulation on the CERMET fuelled reactor. The results (Table 2) show good agreement among the libraries.

Table 2 - Sensitivity analysis on JEFF 3.1 [26]*, ENDF-B-VI-8* [30] *and FENDL 3.0* [31].

	JEFF 3.1	**ENDF-B-VI-8**	**FENDL 3.0**
k_{eff}(-)	1.16791 ± 0.00040	1.15402 ± 0.00042	1.16303 ± 0.00044
β_{eff}(-)	0.00731 ± 0.00016	0.00721 ± 0.00015	0.00719 ± 0.00016
Λ (μs)	39.3 ± 0.2	40.4 ± 0.2	38.0 ± 0.2

The library that returns the highest value of k_{eff} is chosen. In fact, the control of excess reactivity in nominal and accidental scenarios is the most relevant issue for this reactor class, as shown in Section 4.4. The choice of JEFF 3.1 should provide a good conservative margin with respect to the other libraries.

As preliminary consideration, it is worth noting the reflector thickness influence on reactor criticality. The small size of the reactor imposes a minimization of neutrons losses. Furthermore, the beryllium in the reflector also acts as a moderator, with a relevant contribution to neutrons thermalization. In Figure 8 and Figure 9, k_{eff} dependencies on reflector thickness is reported. k_{eff} is not affected by an increase in the radial reflector thickness above a thickness of 20 cm. A similar behaviour is depicted for an axial reflector thickness above 25 cm. Therefore, increasing reflector thickness above those values does not improve the neutronics performance, but adds unnecessary mass to the system. The strong thermalizing effect of the reflector can be deduced from the high thermal flux at the core boundary (Figure 10). The thermal flux in the peripherical region is approximately twice the thermal flux in the inner region. This feature is convenient for reactor operations. Since the CD are located at the core periphery, the B_4C absorber can reduce effectively the thermal flux to control the reactor. On the contrary, limiting the thermal flux in the inner region is much harder, because of the absence of active control component close to the core centre. This last issue becomes evident during submersion accidents.

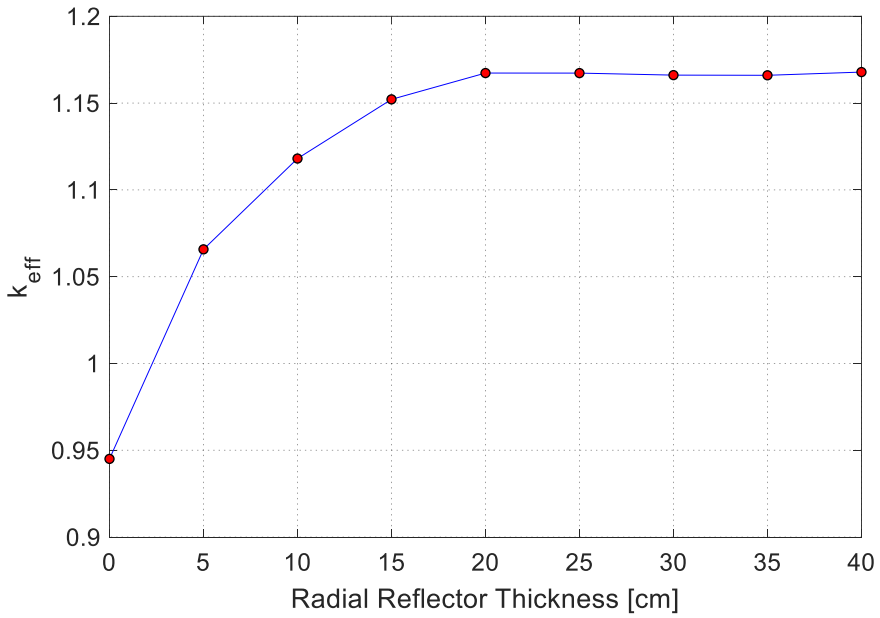

Figure 8 - k_{eff} as a function of radial reflector thickness (σ=20 pcm).

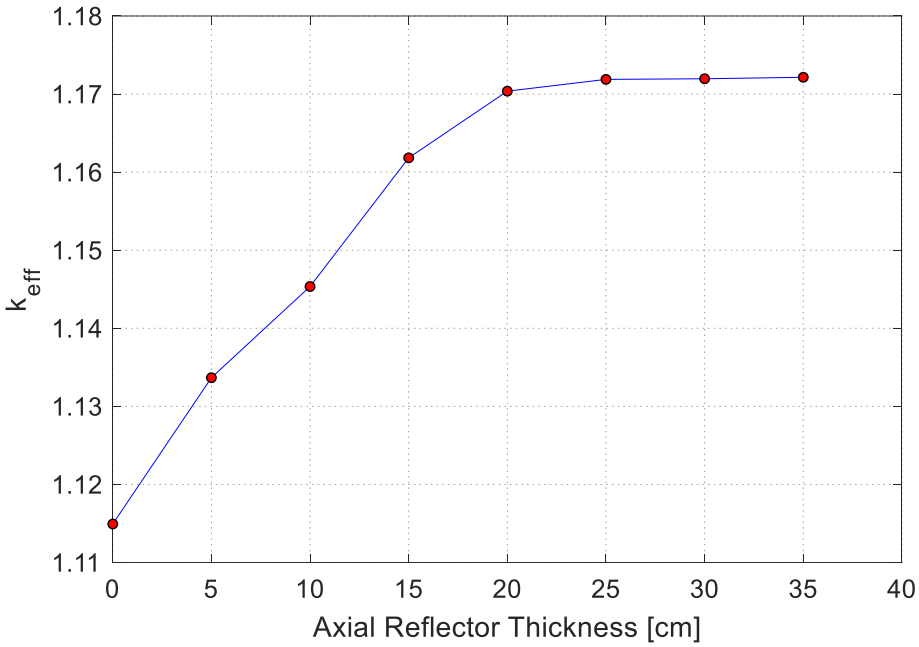

Figure 9 - k_{eff} as a function of axial reflector thickness (σ=20 pcm).

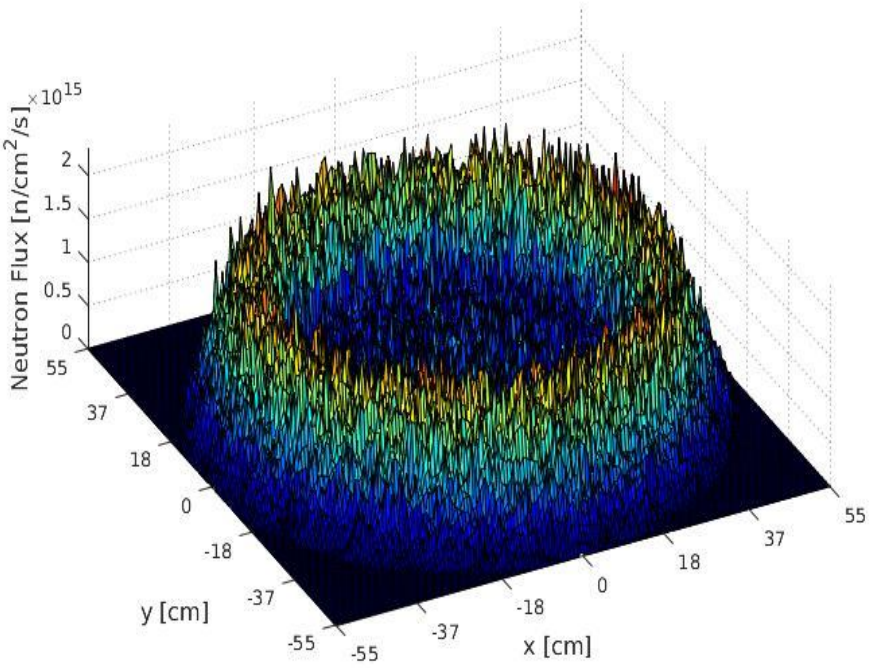

Figure 10 - Thermal neutron flux at core midplane z=0.

Since the reflector contributes for most of the reactor weight (Table 3), minimizing its dimension is an effective way to reduce both reactor mass and excess reactivity. The need for a reduction of the excess reactivity is evident: with an excess reactivity of 27.4 $ and a CD reactivity worth of 20.2 $, the reactor cannot be controlled. The CD reactivity worth is evaluated by simulating the system with the CD fully rotated inward and outward, computing the k_{eff} difference between the two configurations. While β_{eff} can be considered satisfactory, providing a large margin to prompt criticality, the excess reactivity must be minimized. As

already stated, a possible way to do so is the reduction of reflector thickness. Even if at first glance this looks like the best solution, safety requirements limit this approach. The exact behaviour of the reactor in accidental scenarios is described in detail in Section 4.4: the crucial outcome is that the lower the reflector thickness, the larger the reactivity insertion during accidental events. Thus, the excess reactivity minimization should be tackled from the fuel viewpoint, reducing the enrichment and optimizing the division in enrichment zones. The minimum value of excess reactivity required to operate the reactor for the whole mission time has been quantified by a burnup analysis. For a 2 h mission time [27], the excess reactivity required is 200 pcm. If the mission time is increased up to 24 h, the excess reactivity required is approximately 3600 pcm.

Table 3 - CERMET reactor configuration, main results.

	CERMET reactor
k_{eff}	1.16791 ± 0.00040
Re in fuel coating $[at\%]$	5%
Excess reactivity [$]	27.4
β_{eff}	0.00731 ± 0.00016
CD reactivity worth [$]	20.2
Shutdown margin [$]	Not Available
Hot channel factor	2.04
Total mass (without shielding) [Kg]	2756

4.3 Optimization

The optimization through the explorative algorithm described in Section 2 was applied to the base CERMET configuration. To explore the widest area in the domain of possible configurations, the main parameters have been changed in the largest reasonably ranges. The largest reasonably ranges have been obtained as described in Section 2.4 and in the Appendix:

- Axial and radial reflector thickness initially vary in the range [5 cm; 35 cm], with 5 cm steps. Following the first two batches, the range was reduced to [5 cm; 25 cm]. However, 25 cm was removed manually due to the small increase on the excess reactivity it provides;
- The enrichment zones number initially vary in the range [2; 7]. Following the first 6 batches, the range was reduced to [5; 7];
- The maximum initial fuel enrichment varies in the range [7%; 20%]. Following the first batch it is reduced to [12%; 20%]. Below this lower bound, the fissile mass inside the core is not sufficient to achieve criticality;
- Fuel enrichment from one zone to the adjacent differs by 1% or 2%. Larger steps lead to higher peaking factors;

As a first approach, both the nominal operation and the accidental scenarios were simulated by the optimization algorithm. However, this approach was quickly understood to be highly inefficient, leading to a

large number (20 for each configuration, due to the many SSA tested) of meaningless simulations. Indeed, from the results of the nominal conditions one can easily infer whether the reactor will reach supercriticality in accidental scenarios or not. If the excess reactivity or the hot channel factor is already too large in nominal conditions, there is no reason to simulate accidental conditions for that reactor configurations. Thus, the optimization algorithm was modified to run the safety simulations only for the most promising configurations.

To efficiently visualize all the configurations in a suitable space, a scatter plot with the hot channel factor F_{HC} and k_{eff} as axis is chosen (from Figure 11 to Figure 14). Figure 11 shows the results for a huge group of simulations from 4 batches (4x100 simulations). The points are spread over a large range of $k_{eff} = 0.85 \div 1.15$ and $F_{HC} = 2 \div 3.7$, highlighting a huge variability of the results from the input parameters. At the beginning, the enrichment is chosen in the [7%; 20%] range. As the 4 batches are simulated, they are reduced to the aforementioned ranges. Instead, the reflector thickness has been already reduced by the optimization algorithm to [5cm; 20cm] after the run of 2 initial batches. Results from the initial range of reflector thickness are not reported. In fact, the reflector thickness range [25cm; 35cm] leads to configurations with similar values of k_{eff} and F_{HC}, which provide no additional insights and make the post-processing harder due to the much denser results. Figure 12 shows the same results of Figure 11 following a clustering procedure. The k-means algorithm has been applied to find the four more relevant clusters. The total sum of distances s (i.e., the sum of the distance between any point belonging to a cluster and the corresponding centroid) for k = 4 is 44. Each cluster is quite limited in the F_{HC} values, while it has a large variability in the k_{eff} range. The leading input parameter is the radial reflector thickness. Cluster A is mainly populated by configurations that feature a radial reflector thickness of 10 or 15 cm. In cluster B most of the configurations present a radial reflector thickness of 5 or 10 cm, while cluster C contains configurations with a radial and axial reflector thickness of 20 cm. Cluster D is more balanced in terms of radial reflector thickness. As expected, the radial reflector thickness limits the maximum k_{eff} achievable. Very few configurations with a 5cm-thick radial reflector reaches a $k_{eff} = 1.05$, and the 10cm-thick radial reflector is limited to $k_{eff} < 1.10$. The effect of different axial reflector thicknesses is less evident, because of the absence of a bottom axial reflector. Any variation of the axial reflector thickness affects the upper core region only, leading to smaller changes in k_{eff}. The different number of enrichment zones spreads the clusters over the F_{HC} axis, while different fuel enrichments spread the clusters over the k_{eff} axis.

From the optimization viewpoint, cluster B can be considered the optimal region: F_{HC} is the lowest among the different clusters, whereas the excess reactivity is not too large. A small excess reactivity is indeed desirable from the safety viewpoint (see Section 4.4). Cluster A can be regarded as a sub-optimal region: k_{eff} is still limited below critical values for safety purposes, but the higher hot channel factor implies worse rocket performances. The goal of the optimization procedure is reducing the design space such that the cluster B region is explored deeper.

Figure 13 shows the result of the last 3 batches. The improvements provided by the optimization are evident. F_{HC} ranges between 1.8 and 2.8, while k_{eff} ranges between 0.96 and 1.06. There are still a significative number of configurations that cannot operate ($k_{eff} < 1$). They are the result of a trade-off between the lower enrichment input value and the extension of the design space to analyse. If the lower enrichment value is increased, those configurations may be removed, but the fissile mass in the reactor increases. A lower bound of 12% seems a reasonable input value. Figure 14 shows the clusters resulting from these configurations. A total sum of distances of 29 is found for two clusters, while for a single cluster $s = 52$. This means that cluster B (Figure 12) has been almost isolated by the optimization procedure.

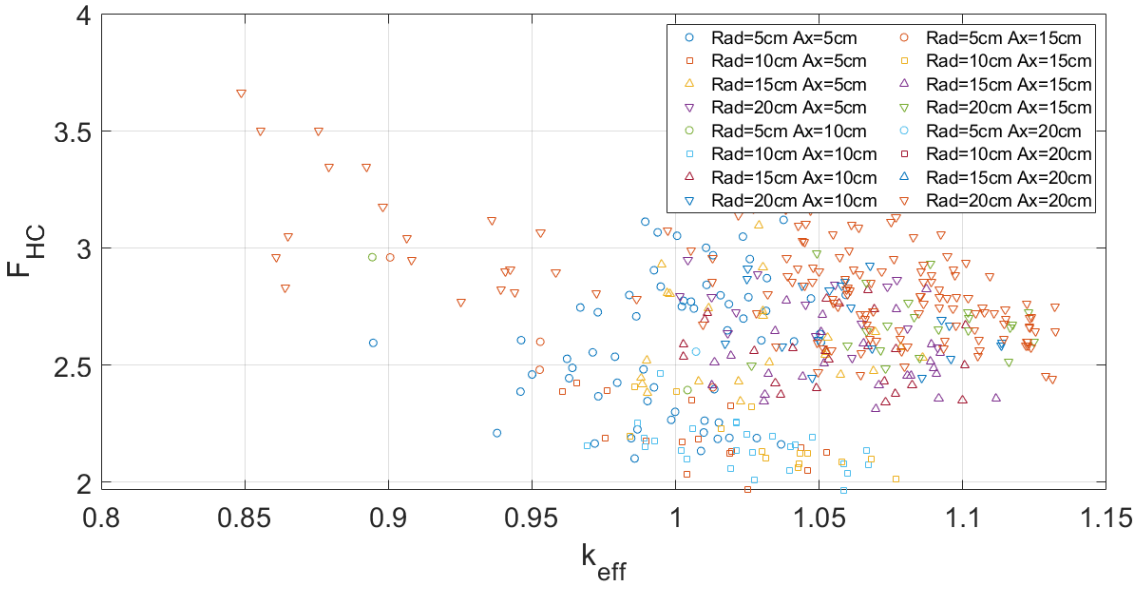

Figure 11 - k_{eff} and F_{hc} for 400 reactor configurations from 4 batches. Results refer to simulations with input parameters weakly optimized. "Rad" stands for radial reflector thickness and "Ax" stands for axial reflector thickness.

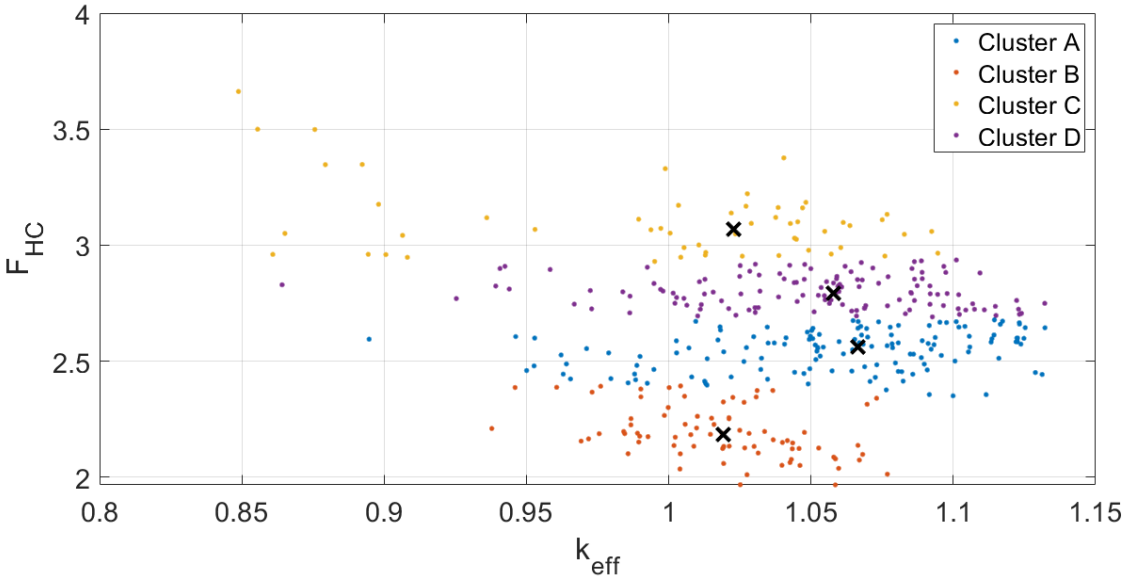

Figure 12 – Clustering of the results shown in Figure 11. Four clusters are identified by a k-means algorithm.

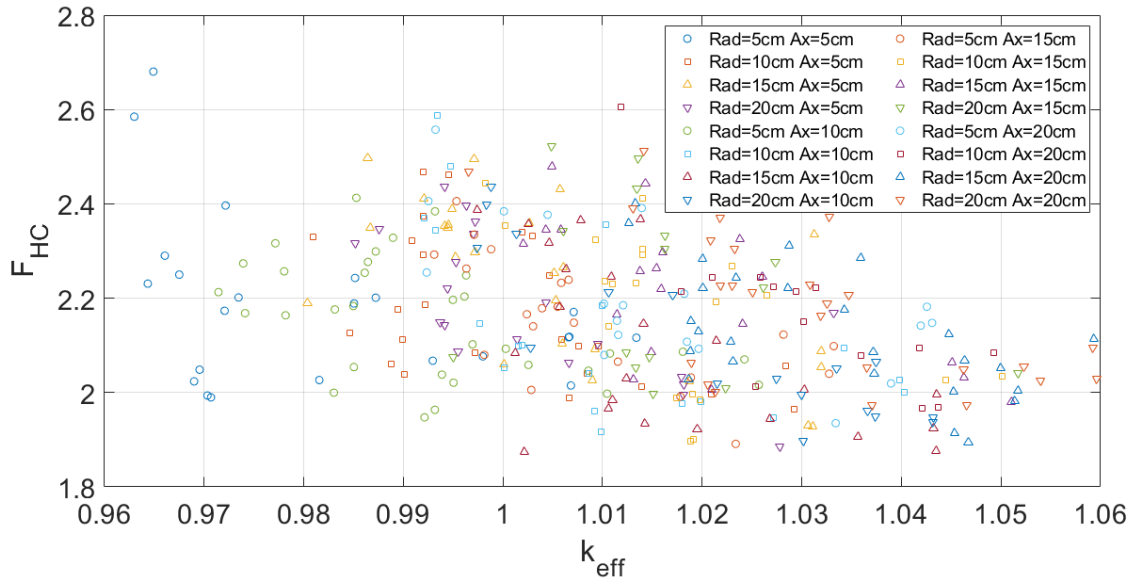

Figure 13 - k_{eff} and F_{hc} for 300 reactor configurations from the 3 last batches. Results refer to simulations with input parameters highly optimized. "Rad" stands for radial reflector thickness and "Ax" stands for axial reflector thickness.

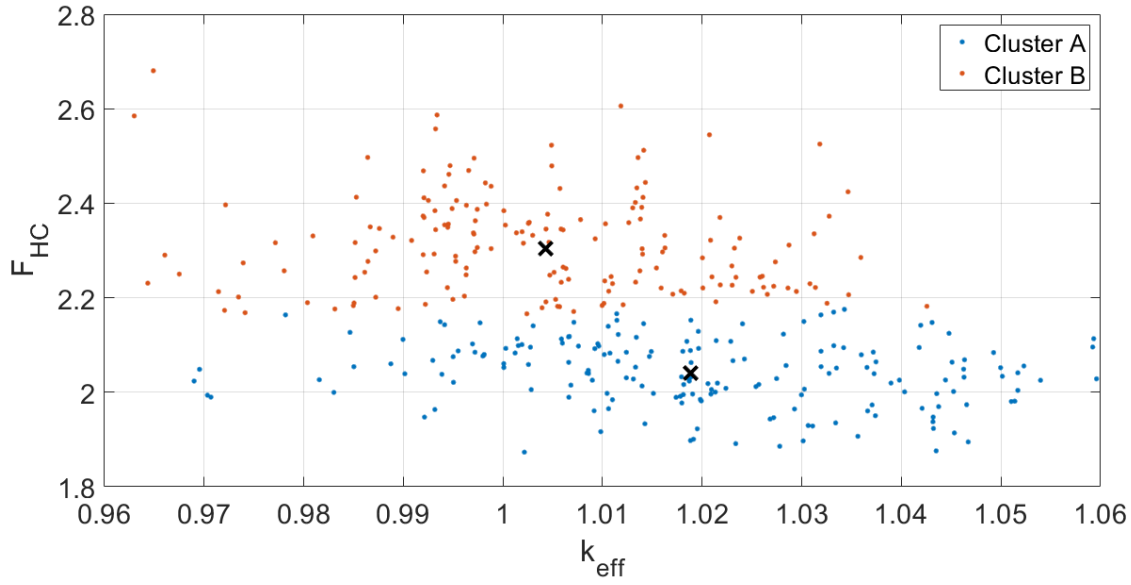

Figure 14 - Clustering of the results shown in Figure 13. Two clusters are identified by a k-means algorithm.

Safety and thermal-hydraulics analyses have been run for the configurations shown in Figure 13, according to the selection procedure described in Section 3. Among all these configurations, the most promising (Table 4) shows a consistent mass saving, a moderate excess reactivity which allows reactor control, and a slightly better F_{HC} if compared to the standard configuration. The results for the safety and the thermal-hydraulics analysis presented in Section 4.4 and Section 4.5 refer to this configuration.

Table 4 - Optimized configuration for the CERMET reactor.

	Optimized configuration
k_{eff}	1.05855 ± 0.00040
Excess reactivity [\$]	9.64
β_{eff} $[-]$	0.00712 ± 0.00010
Λ $[\mu s]$	22
Enrichment zones (% $U235$ enrichment)	7 $([19\ 18\ 17\ 16\ 15\ 14\ 13])$
Reflector thickness (radial/axial) $[\mathrm{cm}]$	$10/10$
Hot channel factor $[-]$	1.96
$U235$ mass saving (%)	7.6
Axial reflector mass saving [Kg]	$94\ (-56\%)$
Radial reflector mass saving [Kg]	$588\ (-60\%)$
Total mass [Kg]	$2074\ (-25\%)$

4.4 Safety analysis

In this section the four accidental scenarios previously introduced are analysed, highlighting reactor weakness to specific class of scenarios. In a submersion in dry sand scenario, the reactor is assumed to be surrounded by a sphere of 5 m radius made of sand (SiO_2 with 30% porosity, $\rho = 1.855\ \mathrm{g/cm^3}$), while moderator and fuel channels remains empty. This is the less dangerous scenario, because no moderation is added in the inner region of the core. It is not the case for the wet sand (SiO_2 with 30% porosity, voids filled by H_2O, $\rho = 2.162\ \mathrm{g/cm^3}$) scenario, in which seawater floods the channels, leading to a much larger reactivity increase. Submersion in seawater (3 wt% NaCl in H_2O, $\rho = 1.025\ \mathrm{g/cm^3}$) shows small differences with the wet sand scenario, while the reflector dismantled scenario results in the hardest scenario to be handled: water filling the channels in the core inner region strongly thermalizes the neutrons in that zone (Figure 15), with a consequent increase of the local power and k_{eff}.

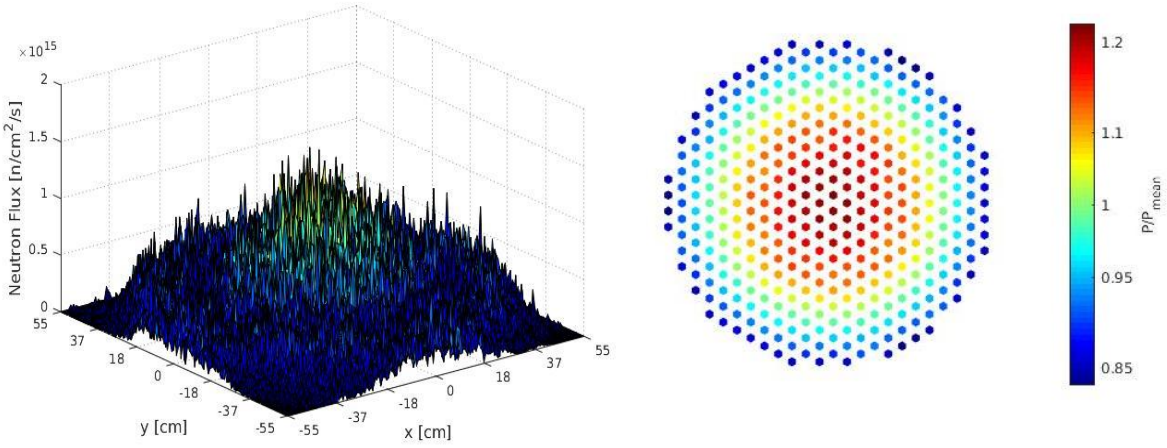

Figure 15 - Thermal neutron flux and power distribution following an accidental scenario – CEREMET optimized configuration.

The thermal neutron flux and power distribution are completely different to the nominal operations case. The B_4C absorbers in the CD cannot act effectively in this situation because the neutron flux peak is too far from the core boundary, and supercriticality is reached (Table 5). This situation gets worse when the reflector is lost due to the impact. In fact, the water surrounding the core acts as moderator and reflector, but the B_4C absorbers are lost. Therefore, as the reflector is dismantled, there is a loss in neutron absorption capability which is not balanced by a loss in reflection and moderation.

Table 5 - k_{eff} following submersion accident. CERMET optimized configuration.

	CD position	**Channels**	**Reflecting medium**	k_{eff}
Submersion in dry sand	Inward	Empty	Sand	1.04746 ± 0.00060
Submersion in wet sand	Inward	Water	Sand	1.20173 ± 0.00060
Submersion in seawater	Inward	Seawater	Seawater	1.20040 ± 0.00060
Reflector dismantled	NA	Seawater	Seawater	1.20794 ± 0.00060

With no further improvement, the reactor reaches supercriticality in all the submersion accidents simulated. Hence, an additional safety system is required. The main options considered are spectral shift absorbers, control rods and an advanced CD system.

4.4.1 Spectral shift absorbers

The SSA absorption cross section is maximum at medium energy, in the epithermal region. If their concentration is tuned properly, SSA depletion follows fissile materials burnup, ensuring an almost constant reactivity. Furthermore, in submersion accidents, moderation addition is directly compensated by an increased neutron absorption provided by the SSA, keeping the reactor subcritical. This mechanism works extremely well with fast spectrum reactors, because in nominal operations the SSA absorptions are almost

negligible. For some reactor design, it is even possible to assist to a reactivity inversion when the reactor gets submerged [32]. Conversely, reactivity issues in nominal operations arise when this solution is brought to thermal reactors (Figure 16).

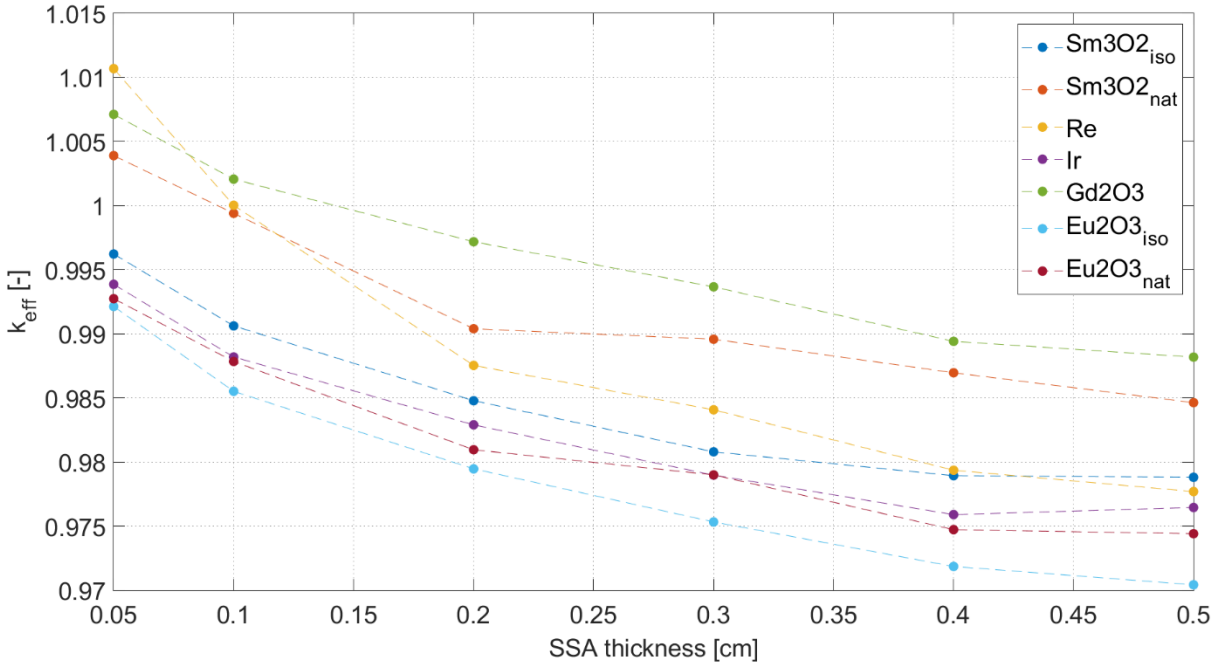

Figure 16 - Effect of different SSA on reactor reactivity (nominal operations) as a function of SSA sleeve thickness.

Samarium and Europium were tested both in their natural isotope and their high-absorbing isotope. For the most absorbing materials even a 0.05 cm sleeve (Figure 17) around the core leads to a subcritical reactor in operating conditions. Other SSA may be implemented as 0.1 cm sleeve, but their contribution in accidental scenarios is still not sufficient to ensure subcriticality. Again, the reason for this behaviour lays in the neutron thermal flux distribution. The SSA sleeve has a strong impact in nominal operations, because the absorbers are located at the peripherical region, where the thermal flux is maximum. When the reactor faces a submersion accident, the thermal neutron flux increases in the inner region, and the SSA absorption is less effective. Results from the configuration that returns the lowest value of k_{eff} are shown in Table 6. It is evident that a SSA sleeve cannot meet safety requirements.

Table 6 - k_{eff} following submersion accidents. Comparison between the configuration with SSA and without SSA.

				No SSA	With SSA
	CD position	**Channels**	**Reflecting medium**	k_{eff}	
Submersion in dry sand	Inward	Empty	Sand	1.04746 ± 0.00060	1.00206 ± 0.00060
Submersion in wet sand	Inward	Water	Sand	1.20173 ± 0.00060	1.12532 ± 0.00060
Submersion in seawater	Inward	Seawater	Seawater	1.20040 ± 0.00060	1.16477 ± 0.00060
Reflector dismantled	NA	Seawater	Seawater	1.20794 ± 0.00060	1.16651 ± 0.00060

SSA dispersion inside the fuel is not effective as well, hence a layer of SSA inside the moderator elements (Figure 17) was investigated. The most effective SSA is found to be rhenium, with a layer of 50 μm between the Zircaloy cladding and the $ZrH_{1.8}$ moderator. This configuration has low impact on nominal operations, both for the small quantity of SSA added to the core and its location. Also, it strongly reduces reactivity in accidental scenarios: being the SSA close to the coolant channels, it is extremely effective when the seawater fills the channels, absorbing most of the thermalized neutrons. The combination of Re layer and CD ensure safety for the dry and wet sand submersion accident, with a core that is slightly supercritical in case of submersion in seawater ($k_{eff} = 1.01003$). The $1000\,pcm$ excess reactivity from the last case can be absorbed with additional tuning, but the reflector dismantled case is still an open issue, with a $k_{eff} = 1.12600$.

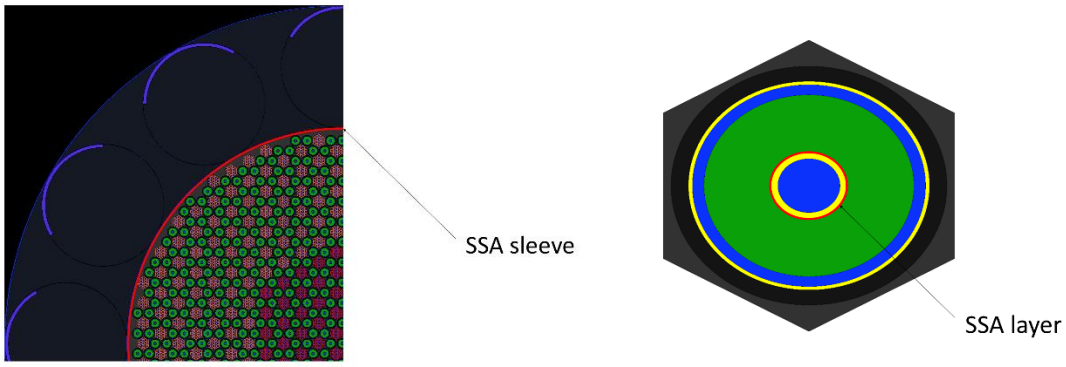

Figure 17 - Reactor configuration with SSA (in red). Left: SSA implemented as a sleeve around the core. Right: SSA implemented as a layer in the moderator elements. SSA thickness not in scale.

4.4.2 Control rods

To face this last class of accidents the introduction of control rods is analysed: this choice increases system complexity, but it is worth to understand the reactor response to large, negative reactivity insertion. An increasing number of control rods made of B_4C was inserted inside the core, replacing fuel elements, up to 7: this is the minimum number of control rods required to ensure subcriticality in the worst-case scenario. Their position was chosen arbitrarily (Figure 18), in the sense that no sensitivity analysis was performed to find the better location for each one. However, since one is placed in the middle and the remaining six at half the core radius, 60 degrees spaced, one may expect little variations from the obtained results (Table 7).

Table 7 - k_{eff} following submersion accidents, reactor configuration with control roads

	CD position	**Channels**	**Reflecting medium**	$\boldsymbol{k_{eff}}$
Submersion in dry sand	Inward	Empty	Sand	0.95440 ± 0.00060
Submersion in wet sand	Inward	Water	Sand	0.99819 ± 0.00060
Submersion in seawater	Inward	Seawater	Seawater	0.99412 ± 0.00060
Reflector dismantled	NA	Seawater	Seawater	0.99348 ± 0.00060

From a theoretical viewpoint, control rods are an effective system to maintain the reactor under safe conditions even in the worst accidental scenario. Shutdown margin may be increased by adding another rod or by optimizing safety rod design and position. Nonetheless, introducing moving rods in a nuclear thermal rocket with a solid core poses engineering challenges. Failure of both control rods and CD system should be investigated because an impact strong enough to dismantle the reflector could reasonably damage the control rods moving mechanism as well. If these two systems fail, the situation is not much different from a core with the reflector dismantled and without control rods. This is the reason that leads to the analysis of an advanced CD system.

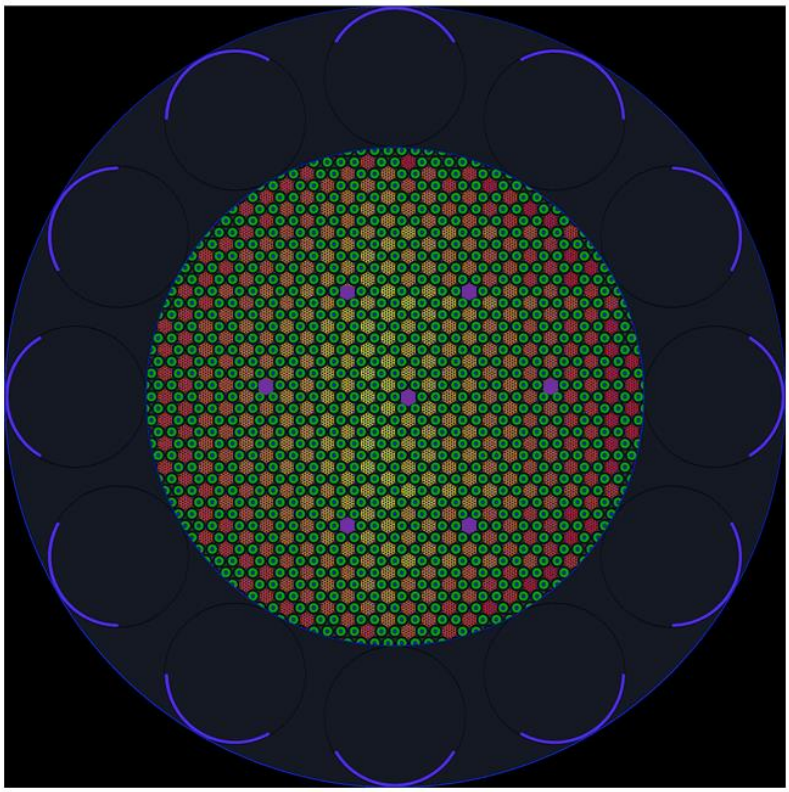

Figure 18 - Poloidal cross section of the core after the control rods insertion. Control rods are represented in purple. Each control rod replaces a hexagonal fuel element.

4.4.3 Advanced control drum system

The most important outcome from the previous analysis is that no matter how much negative reactivity can be inserted following a submersion accident, there is always the probability that the reactor becomes supercritical. Thus, the problem should be tackled from a different direction: the underlying idea is to make control drums indispensable components for reactor criticality. This translates in fuel addition to the CD and a shifting toward the core centre. An advanced CD system has been already proposed [19], though not widely analysed in literature. From the previous neutronics analysis it was found that increasing absorber thickness in the CD above a certain value has no effect on core neutronics, because of the peripherical location occupied by CD. Once they are moved closer to the inner region of the core, absorbers thickness is increased up to 4 cm, to provide a much relevant negative reactivity insertion. Concerning the fuel and the moderator layers, moderator occupies three sectors with the following inner and outer radii: 9cm/8cm,7cm/6 cm, 4.5cm/4cm (Figure 19). The zones between moderator layers are filled with fuel 20% enriched: this configuration helps to maximize the CD reactivity contribution. This solution results in the optimal one, with a huge shutdown margin (Table 8) for each case. The reactor is kept subcritical even following a submersion accident with reflector dismantling, providing about $-2\$$ of shutdown margin.

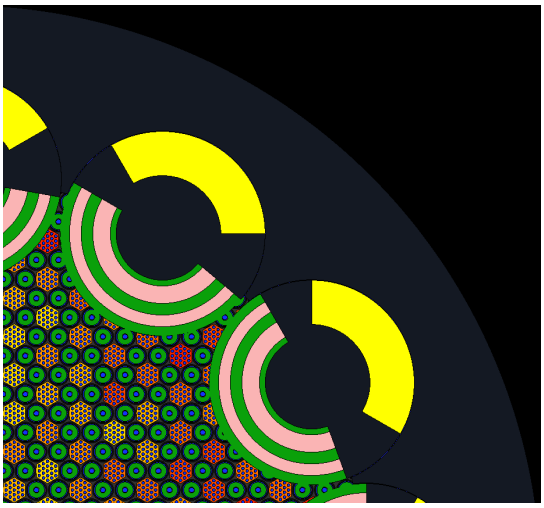

Figure 19 - Detail of the poloidal cross section showing the accident tolerant control drums [19]. *Green and pink circular sectors represent moderator and fuel, respectively. The yellow sector represents the B_4C absorber with increased thickness.*

Table 8 - k_{eff} following submersion accidents, reactor configuration with an advanced CD system.

	CD position	**Channels**	**Reflecting medium**	k_{eff}
Submersion in dry sand	Inward	Empty	Sand	0.84227 ± 0.00040
Submersion in wet sand	Inward	Water	Sand	0.95294 ± 0.00040
Submersion in seawater	Inward	Seawater	Seawater	0.95031 ± 0.00040
Reflector dismantled	NA	Seawater	Seawater	0.98564 ± 0.00040

4.5 Thermal-hydraulics analysis and rocket performances

A safe reactor with enough excess reactivity to ensure operability for the whole mission time is the main target from the neutronics and safety viewpoint. However, rocket performances must be evaluated, to assess the efficiency of the whole methodology described in Section 2. Furthermore, the temperature profile in the hot channel must be computed to check whether thermal limits are exceeded in any location of this channel. Preliminary results from hot channel analysis shew a criticality on fuel temperature, being the melting temperature (3000 K) exceeded, with a peak temperature of 3576 K. A cosine power profile was initially assumed. Since the fuel temperature in the average channel has a suitable margin to the melting temperature, an ideal orificing may lead to a rebalance of the temperature in the core. In addition to that, the cosine power profile reveals to be not suitable for this reactor configuration. Indeed, the absence of a bottom reflector makes the power profile q' strongly asymmetric (Figure 20). Thus, the real power profile is considered. The mass flow rate among the channels is tuned until the fuel temperature in the hot channel drops below 3000 K. The additional mass flow rate in the hot channel is provided by the other channels, which experience a temperature increase due to the decrease in coolant flow rate. This operation leads to a fuel temperature of 2829 K in the average channel and 2996 K in the hot channel (Table 9), with a mass flow rate increase of 15% in the hot channel.

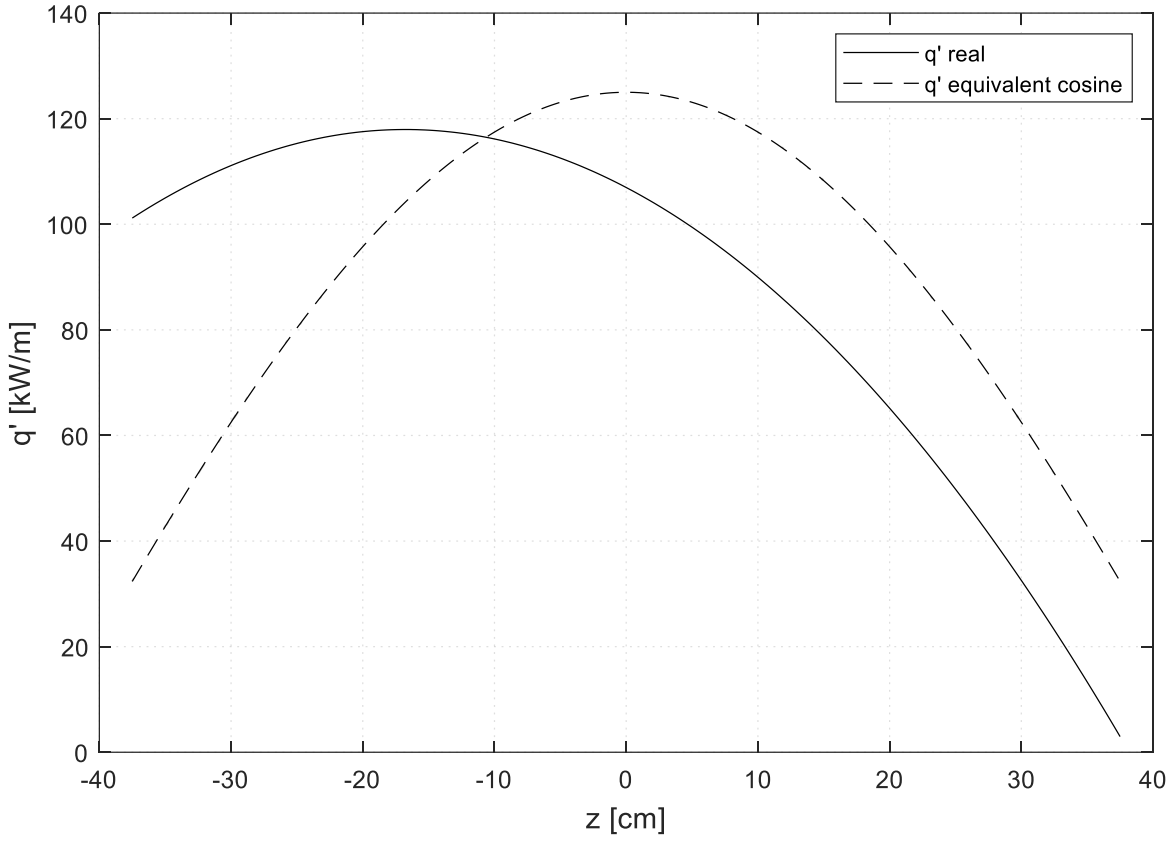

Figure 20 - Hot channel axial power profile per unit length.

Table 9 - Thermal-hydraulics analysis results for the real power profile. Core with inlet orifice.

	Core with inlet orifice
Hot channel mass flow rate [kg/s]	$2.0 \cdot 10^{-3}$
Peak temperature in the hot channel [K]	2996
Peak temperature in the average channel [K]	2829
Outlet coolant temperature (average channel) [K]	2661

Finally, rockets performances are evaluated through basic rockets science formulae. The thrust is computed as:

$$F_{thrust} = \dot{m}_{tot} \cdot u_{exit}$$

where u_{exit} is the coolant (propellant) average exit speed. In vacuum, u_{exit} can be found as:

$$u_{exit} = \sqrt{\frac{T_c \cdot R}{MM} \cdot \left(\frac{2\gamma}{1-\gamma}\right)}$$

where T_c is the combustion chamber gas temperature, here assumed equal to the core outlet coolant temperature, R is the universal gas constant, MM is the molecular mass of the gas and γ is the isentropic coefficient. The specific impulse is computed as $I_{sp} = \frac{F_{thrust}}{g \cdot \dot{m}}$, where g is the gravity acceleration at Earth's surface. A comparison (Table 10) with the reference configuration shows the huge improvement that the whole optimization procedure provides. Specifically, despite the larger mass, the thrust to weight ratio is larger for the present configuration, thanks to a significative increase in rocket thrust.

Table 10 - Rocket performances. Comparison between C-LEU-NTR and the optimized configuration with an advanced CD system.

	C-LEU-NTR	**Advanced CD system reactor configuration**
Reactor mass [kg]	2016	2226
Ex-core components mass (assumed) [kg]	1000	1000
Thrust [kN]	110	122
Specific impulse [s]	900	996
Thrust to weight ratio - reactor only	$N.A.$	5.6
Thrust to weight ratio - reactor and ex-core components	3.49	3.85

5. Discussion

The results in the previous section have been presented in the most convenient way for the reader: however, it is worth to describe deeper the approach followed. The Serpent model for the composite fuelled reactor was verified by comparison with an existing design available in literature. Then, the composite fuel was replaced by a CERMET fuel. This was considered the base configuration to be optimized. The optimization procedure has been applied for a total of 9 batches of 100 simulations each. At each batch, the algorithm reduced the design space, moving towards an optimal region. The combination of an efficient Python script and the performance metrics brought enormous advantages. Serpent input file generation can be extremely cumbersome and prone to user's errors when dealing with multiple configurations: nevertheless, its textual based input and the MATLAB® readable output are suitable for a complete script automation. Each Serpent simulation requires about 10 minutes to be run with that choice of parameters (Table 4) – on a machine with 8gb RAM and i5 processor 2.3 GHz. The choice of the performance metrics (k_{eff}, F_{HC}, reactor mass) is crucial, since those quantities are the filtering criteria for further simulations. As a matter of fact, simulating all the submersion accidents with all the possible safety systems (7 SSA, control rods and advanced CD system, considering only the optimal thickness for the SSA sleeve) for each configuration would require $3.9 \cdot 10^8\ s$, or $12\ y$. The hierarchical series of constraints demonstrated to be effective, though a tuning of the threshold parameters may improve the methodology. For instance, even during the last batches a huge number of useless configurations ($k_{eff} < 1$) were simulated. Furthermore, some initial full simulations (neutronics, safety and thermal-hydraulics) were required to set the initial values for the threshold parameters, especially the hot channel factor. While the hot channel factor is an effective parameter for the reduction of the design space from the thermal-hydraulics viewpoint, an equivalent parameter was not found for the safety analysis. A link between the excess reactivity in nominal operation and the excess reactivity in accidental scenarios is not evident, due to system complexity.

The relation between reflector thickness and core reactivity was studied in depth: thick reflectors lead to extremely high excess reactivities, at least with the standard enrichment zones (17% inner, 20% outer). Reducing the reflector thickness, both axial and radial, is the most effective way to fulfil two requirements (low mass and low excess reactivity) acting on a single component. This procedure has two main drawbacks, related to the moderating and reflective capability of beryllium in the reflector. In nominal operations, small reflector dimensions lead to a large reduction in reactivity, because of lower moderation in the core and increased leakages. The direct consequence is the necessity to keep fuel enrichment at high values (nearly 20%), cutting the possibility of a fissile mass reduction. The second drawback is related to safety: it was shown (Figure 15) that following a submersion accident the thermal flux peaks move from the core periphery to the inner region, due to the insertion of moderating media (water, sand) in the coolant channels. This behaviour cannot be avoided, due to the very nature of the reactor. However, if a large reflector is designed, the presence of the additional, surrounding medium at reflector boundaries has almost no effect on core neutronics: that is, the reflector thickness is already optimal to minimize neutrons losses. If, instead, the reflector thickness is small, the surrounding reflective medium adds further positive reactivity, which brings the reactor to supercriticality. Ensuring safety for such configurations is extremely challenging. It seems worth to accept reflector thickness slightly larger to obtain significant advantages in failure scenarios. The reflective media (water, sand) have comparable effects on the neutronics when they replace the reflector (the reflector-dismantled scenario). Hence, for a reactor configuration with sufficiently thick reflector, no reactivity insertion is foreseen from the surrounding medium.

Concerning fuel enrichment, two complementary optimizations were performed. The first improvement is a reduction of fuel enrichment, lowering the total mass and the nuclear proliferation risk. The second optimization foresees a more efficient division in enrichment zones: by combining these two procedures the power distribution is flattened, with evident advantages for safety and performances. In fact, a lower hot

channel factor translates in lower fuel temperatures, minimizing the possibility of thermal failures. Furthermore, higher mean coolant temperatures can be achieved, increasing rocket performances.

The last feature of interest is the safety system: spectral shift absorbers (SSA), control rods and an advanced system of control drums were tested. Spectral shift absorbers can be considered passive systems, in contrast with control rods and control drums, which require moving mechanism. This is a desirable feature from the safety viewpoint. However, SSA heavily affect the neutronics during nominal operations: the SSA amount required to reach subcriticality following a submersion accident is so large that the reactor is not critical during nominal operations. Control rods are active systems, leaving no issues in nominal operations. Though, their implementation in a real design should be demonstrated, and the addition of moving components could be considered an avoidable system complication, provided that simpler solutions are available. Concerning the advanced CD system [19]**,** the underlying idea to make the reflector a crucial component for reactor criticality, increasing its reactivity worth, reveals to be effective. Among the solutions explored the advanced CD system deserves further investigations and a proof of concept, looking as a promising technology for future designs.

Finally, the whole procedure would result meaningless if the final configurations had not shown significant improvement. Compared to the base configuration (Table 3 and Table 4), its excess reactivity allows for optimal control in nominal operations and subcriticality accidental situations; the hot channel factor is slightly lower, and the total mass is about 25% less. Compared to the C-LEU-NTR (Table 10), from a rocket performances viewpoint (comparing the reactor itself is meaningless, since the two configurations use different fuels), the optimal configuration shows higher specific impulse and thrust-to-weight ratio, with a slightly larger thrust value.

6. Conclusions

In this work, an optimization approach for a preliminary reactor design for NTP has been proposed and then applied to a LEU, CERMET fuelled reactor. Neutronics, thermal-hydraulics and safety are considered in the analysis, providing a comprehensive view on the reactor features and weaknesses. A systematic procedure to explore and optimize possible reactor configurations was successfully implemented through a Python script which integrates Serpent pre-processing, simulations and MATLAB® post-processing.

The optimization routine effectively reduced the design space to an optimal region, limiting the configurations to be analysed. Compared to the starting configuration, the most promising configuration achieved a 25% system mass reduction, 7.6% fissile mass saving and a lower hot channel factor with consequent better rocket performances. However, the strongest constraints relate to safety. Many promising configurations were discarded because the reactor could not reach subcriticality following a submersion accident. Methodologies for preliminary design should therefore address safety in the early stages of the design. Reducing the design space to limit the configurations to be analysed may be an effective way to tackle the problem.

Future works will focus on the improvement of the procedure to reduce the design space. The series of hierarchical constraints is effective, but not efficient. Unnecessary simulations may be further reduced if the optimization step manages to completely remove the design space region leading to $k_{eff} < 1$. Alternative approaches to the hierarchical constraints will be investigated as well. Specifically, soft computing techniques may overcome some of the weakness of the hierarchical constraints by finding a pattern in the configurations that fulfil safety requirements. From this perspective, the approach presented in the work may be exploited to build a huge database with user defined features to train and test soft computing models.

References

[1] M. A. Gibson, D. I. Poston, P. McClure, T. Godfroy, J. Sanzi, and M. H. Briggs, "The Kilopower Reactor Using Stirling TechnologY (KRUSTY) Nuclear Ground Test Results and Lessons Learned," in *2018 International Energy Conversion Engineering Conference*, American Institute of Aeronautics and Astronautics, 2018, doi: https://doi.org/10.2514/6.2018-4973.

[2] S. K. Borowski, D. R. McCurdy, and T. W. Packard, "Nuclear Thermal Propulsion (NTP): A proven growth technology for human NEO/Mars exploration missions," in *2012 IEEE Aerospace Conference*, Mar. 2012, pp. 1–20, doi: 10.1109/AERO.2012.6187301.

[3] J. E. Fittje, B. G. Schnitzler, and S. Borowoski, "Revised Point of Departure Design Options for Nuclear Thermal Propulsion." 2015, [Online – Last access: October 2020]. Available: https://ntrs.nasa.gov/search.jsp?R=20150007681.

[4] P. J. Husemeyer, V. Patel, P. F. Venneri, W. R. Deason, M. J. Eades, and S. D. Howe, "CSNR Space Propulsion Optimization Code: SPOC," *Proc. Conf. Nuclear and Emerging Technologies for Space, Albuquerque*, New Mexico, 2015.

[5] C. D. Fletcher, "Capabilities of the ATHENA computer code for modeling the SP-100 space reactor concept," No. EGG-RST-7025. EG and G Idaho, Inc., Idaho Falls (USA), 1985. doi: 10.2172/6350103.

[6] N. W. Touran, J. Gilleland, G. T. Malmgren, C. Whitmer, and W. H. Gates, "Computational Tools for the Integrated Design of Advanced Nuclear Reactors," *Engineering*, vol. 3, no. 4, pp. 518–526, Aug. 2017, doi: 10.1016/J.ENG.2017.04.016.

[7] J. M. Taub, "Review of fuel element development for nuclear rocket engines," United States, 1975. [Online - Last access: October 2020]. Available: http://inis.iaea.org/search/search.aspx?orig_q=RN:07220629.

[8] K. Benensky, P. Venneri, and M. Eades, "Survey of Fuel System Options for Low Enriched Uranium (LEU) Nuclear Thermal Propulsion," *Nucl. Emerg. Technol. Sp. 2017*, no. February, pp. 1–12, 2017.

[9] K. Benensky, M. J. Wang, J. Nieminen, M. Eades, and S. Howe, "Preliminary analysis of Low Enriched Uranium (LEU) ultra high temperature nuclear thermal rockets capable of 1100s specific impulse," *Nucl. Emerg. Technol. Space, NETS 2016*, no. April 2018, pp. 93–102, 2016.

[10] R. A. Gabrielli and G. Herdrich, "Review of Nuclear Thermal Propulsion Systems," *Prog. Aerosp. Sci.*, vol. 79, pp. 92–113, 2015, doi: 10.1016/j.paerosci.2015.09.001.

[11] R. H. Frisbee, "Advanced Space Propulsion for the 21st Century," *J. Propuls. Power*, vol. 19, no. 6, pp. 1129–1154, Nov. 2003, doi: 10.2514/2.6948.

[12] B. G. Schnitzler and S. K. Borowski, "Small fast spectrum reactor designs suitable for direct nuclearthermal propulsion," *48th AIAA/ASME/SAE/ASEE Jt. Propuls. Conf. Exhib. 2012*, 2012.

[13] S. Labib and J. King, "Design and analysis of a single stage to orbit nuclear thermal rocket reactor engine," *Nucl. Eng. Des.*, vol. 287, pp. 36–47, 2015, doi: 10.1016/j.nucengdes.2015.02.006.

[14] S. H. Nam, P. Venneri, Y. Kim, J. I. Lee, S. H. Chang, and Y. H. Jeong, "Innovative concept for an ultra-small nuclear thermal rocket utilizing a new moderated reactor," *Nucl. Eng. Technol.*, vol. 47, no. 6, pp. 678–699, 2015, doi: 10.1016/j.net.2015.06.003.

[15] P. F. Venneri and Y. Kim, "A feasibility study on low-enriched uranium fuel for nuclear thermal rockets - I: Reactivity potential," *Prog. Nucl. Energy*, vol. 83, pp. 406–418, 2015, doi: 10.1016/j.pnucene.2015.05.003.

[16] P. F. Venneri and Y. Kim, "A feasibility study on low enriched uranium fuel for nuclear thermal

rockets - II: Rocket and reactor performance," *Prog. Nucl. Energy*, vol. 87, pp. 156–167, 2016, doi: 10.1016/j.pnucene.2015.04.013.

[17] J. C. King and M. S. El-Genk, "Submersion-Subcritical Safe Space (S4) reactor," *Nucl. Eng. Des.*, vol. 236, no. 17, pp. 1759–1777, 2006, doi: 10.1016/j.nucengdes.2005.12.010.

[18] A. E. Craft, R. C. O'Brien, S. D. Howe, and J. C. King, "Submersion criticality safety of tungsten-rhenium urania cermet fuel for space propulsion and power applications," *Nucl. Eng. Des.*, vol. 273, pp. 143–149, 2014, doi: 10.1016/j.nucengdes.2014.01.028.

[19] H. C. Lee, T. Y. Han, H. S. Lim, and J. M. Noh, "An accident-tolerant control drum system for a small space reactor," *Ann. Nucl. Energy*, vol. 79, pp. 143–151, 2015, doi: 10.1016/j.anucene.2015.02.001.

[20] H. C. Lee, H. S. Lim, T. Y. Han, and Š. Čerba, "A neutronic feasibility study on a small LEU fueled reactor for space applications," *Ann. Nucl. Energy*, vol. 77, pp. 35–46, 2015, doi: 10.1016/j.anucene.2014.10.015.

[21] J. C. King, "A Methodology for the Neutronics Design of Space Nuclear Reactors," *AIP Conference Proceedings*. Vol. 699. No. 1. American Institute of Physics, 2004.

[22] J. Leppänen, M. Pusa, T. Viitanen, V. Valtavirta, and T. Kaltiaisenaho, "The Serpent Monte Carlo Code: Status, Development and Applications in 2013," *SNA + MC 2013 - Jt. Int. Conf. Supercomput. Nucl. Appl. + Monte Carlo*, 2014, [Online – Last access: October 2020]. Available: https://doi.org/10.1051/snamc/201406021.

[23] M. J.L. Turner, *Rocket and spacecraft propulsion: principles, practice and new developments*. Springer Science & Business Media, 2008.

[24] A. E. Craft and J. C. King, "Reactivity control schemes for fast spectrum space nuclear reactors," *Nucl. Eng. Des.*, vol. 241, no. 5, pp. 1516–1528, 2011, doi: https://doi.org/10.1016/j.nucengdes.2011.01.049.

[25] "Human Exploration of Mars Design Reference Architecture," SP-2009-566, NASA, 2009.

[26] OECD/NEA Data Bank, "The JEFF-3.1 Nuclear Data Library." 2006, [Online – Last access: October 2020]. Available: http://www.oecd-nea.org/dbdata/nds_jefreports/.

[27] B. G. Drake, S. J. Hoffman, and D. W. Beaty, "Human exploration of mars, design reference architecture 5.0," *IEEE Aerosp. Conf. Proc.*, 2010, doi: 10.1109/AERO.2010.5446736.

[28] S. H. Nam, P. Venneri, Y. Kim, S. H. Chang, and Y. H. Jeong, "Preliminary conceptual design of a new moderated reactor utilizing an LEU fuel for space nuclear thermal propulsion," *Prog. Nucl. Energy*, vol. 91, pp. 183–207, 2016, doi: 10.1016/j.pnucene.2016.02.008.

[29] L. L. Snead and S. J. Zinkle, "Use of Beryllium and Beryllium Oxide in Space Reactors," *AIP Conf. Proc.*, vol. 746, no. 1, pp. 768–775, Feb. 2005, doi: 10.1063/1.1867196.

[30] Cross Section Evaluation Working Group, "ENDF/B-VI Summary Documentation, Report BNL-NCS-17541 (ENDF-201)," National Nuclear Data Center, Brookhaven National Laboratory, Upton, NY, USA., 1991.

[31] R. A. Forrest *et al.*, "FENDL-3 Library. Final Report of the Coordinated Research Project on Nuclear Data Libraries for Advanced Systems: Fusion Devices." 2013, Accessed: May 11, 2020. [Online – Last access: October 2020]. Available: https://inis.iaea.org/search/search.aspx?orig_q=RN:45029183.

[32] J. C. King and M. S. El-Genk, "Submersion criticality safety of fast spectrum space reactors: Potential spectral shift absorbers," *Nucl. Eng. Des.*, vol. 236, no. 3, pp. 238–254, 2006, doi: https://doi.org/10.1016/j.nucengdes.2005.07.005.

Appendix

Simulation inputs

In this appendix, the input values for the simulations are reported for readers' convenience (Table 11 and Table 12). The geometrical values in Table 12 refers to the starting CERMET configuration. These values have been modified to get to the final optimized configuration as described in the work.

Table 11 - Serpent simulation input parameters. Multiple values refer to [base configuration / optimized configuration / explorative simulations].

General settings	
Neutron population	50000/ 50000 / 20000
Active cycles	100 / 100 / 50
Inactive cycles	50 / 50 / 25
Reactor power [MW]	450
Boundary condition	Vacuum

Table 12 - Serpent geometrical input parameters for the initial reactor core configuration.

Geometrical input	
Outer core radius (cm)	35
Inner core radius (cm)	15.4
Core height (cm)	75
Axial reflector thickness (cm)	20
Lower plenum height (cm)	2.5
Radial reflector outer radius (cm)	55
B_4C thickness (cm)	0.5
Control drum radius (cm)	9.9
Inner and outer coolant ring thickness (cm)	0.15

All the figures in the appendix have been obtained through the *plot* option in Serpent. The reactor poloidal cross section is reported in Figure 21. It is possible to distinguish the inner fuel zone (red fuel elements), the outer fuel zone (pink fuel elements) and the control drums installed in the radial reflector. The inner fuel elements, which would get cut by the inner core radius, have been adjusted to avoid fuel elements with mixed enrichment.

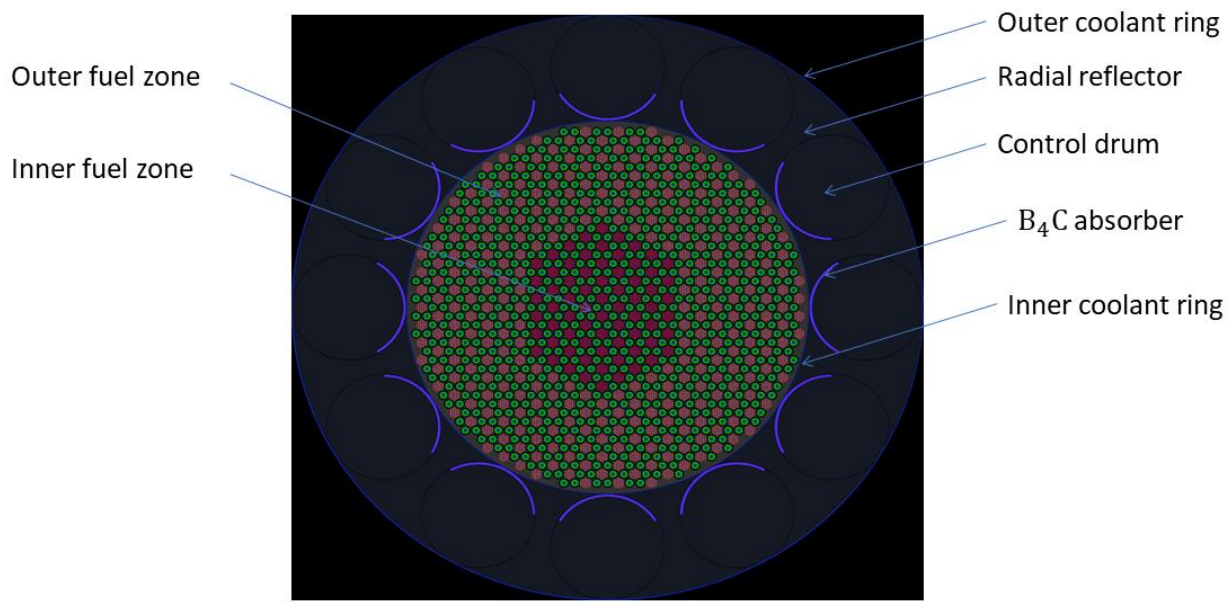

Figure 21 - Poloidal cross section of the reactor core, at midplane. The main components are depicted.

A zoom of the outer zone of the poloidal section is reported for readers' convenience. Note that the elements that would have been cut on the boundaries have been completely removed, and graphite is placed instead.

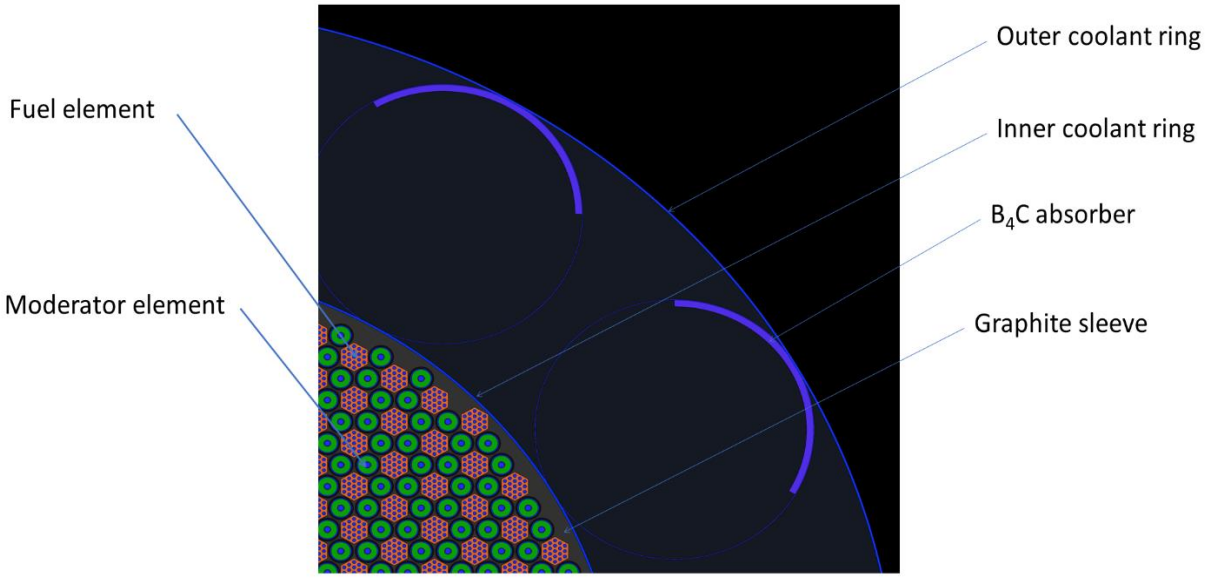

Figure 22 - Detail of the reactor poloidal cross section at midplane, showing the control drum design.

The axial cross section is reported in Figure 23. Note that there is not an upper plenum, but a lower plenum only.

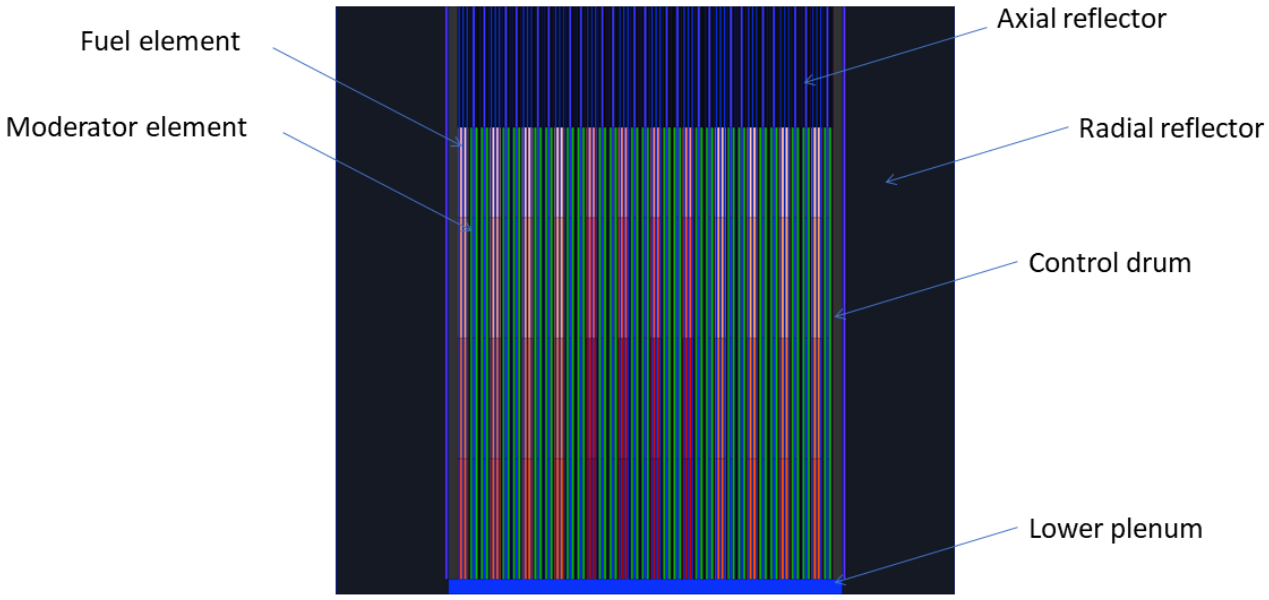

Figure 23 - Axial core cross section. The different fuel colours in the axial direction refer to different temperature zones.

The active core has been divided in four temperature zones (Figure 24, Table 13), to consider temperature effects. A mean temperature for each zone is assigned. In principle, a larger number of zones may be defined, but four temperature zones are enough for the purpose of the work. The four inner elements (darker colours) belong to the inner enrichment zone.

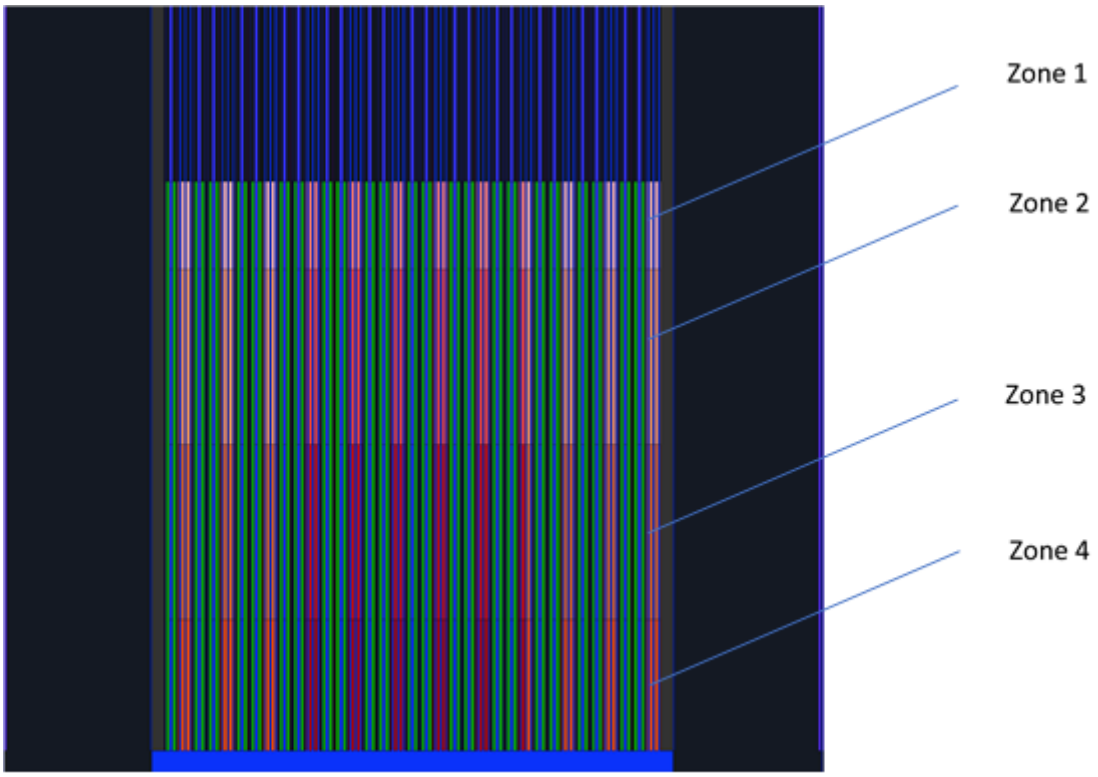

Figure 24 – Axial cross section of the core. The temperature zone division is depicted.

Table 13 - Axial zone division. Temperatures and height for each zone.

	Height [cm]	**Coolant temperature in fuel channels [K]**	**Coolant temperature in moderator channels [K]**	**Fuel temperature [K]**
Zone 1	15	900	120	1000
Zone 2	20	1500	220	1600
Zone 3	20	2300	300	2400
Zone 4	20	2650	450	2750

The hexagonal fuel element presents 19 coolant channels, distributed as in Figure 25. The fuel matrix is made of CERMET, as described in the paper.

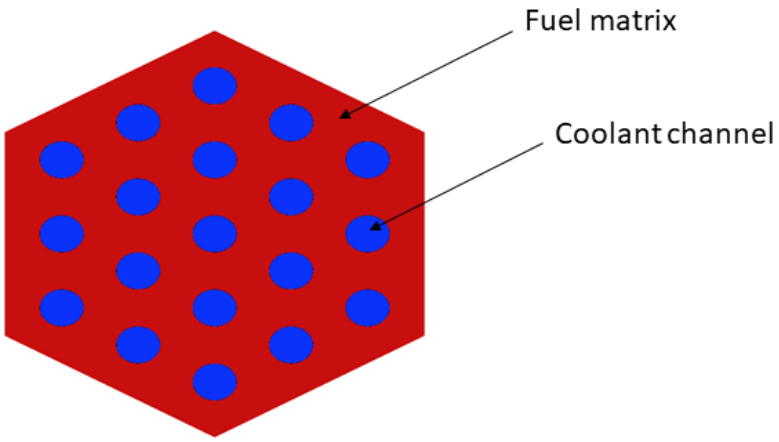

Figure 25 - Hexagonal fuel element. The fuel matrix is in red, the 19 cooling channels in blue.

The relevant geometrical dimensions for the fuel are reported in Table 14. The equivalent fuel radius is the one defined for the thermal-hydraulics analysis.

Table 14 - Fuel element data

Number of coolant channel	19
Channel radius [cm]	0.12292
Fuel coating thickness [cm]	0.00508
Flat-to-flat distance [cm]	1.905
Equivalent fuel radius [cm]	0.2295

Concerning moderator elements, each material outer radius is reported both in Figure 26 and in Table 15 for reader's convenience.

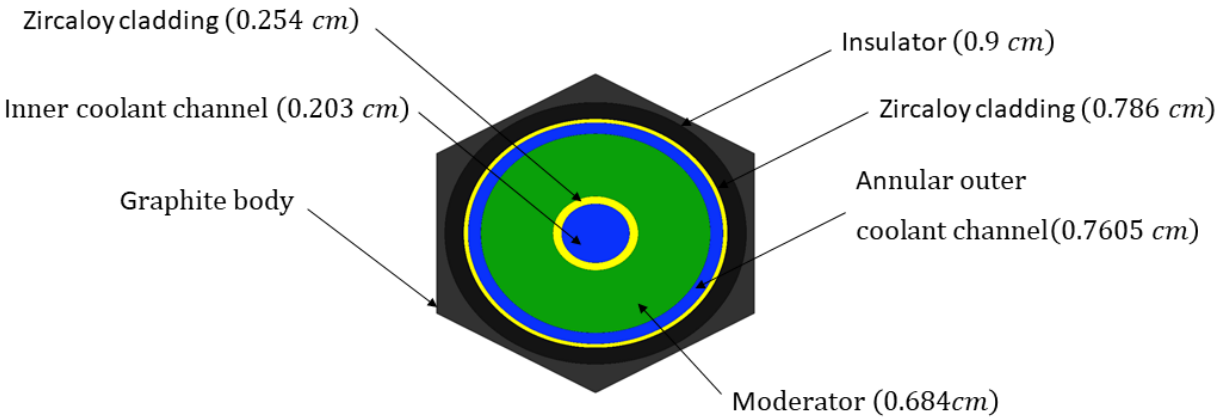

Figure 26 - Hexagonal moderator element. The outer radius of each cylindrical component is reported in bracket. The colour legend is the following: Graphite body (grey), thermal insulator (black), Zircaloy (yellow), moderator (green), coolant (blue).

Table 15 - Moderator element geometrical parameters

Component	**Outer radius [cm]**
Inner coolant channel	0.203
Zircaloy cladding	0.254
Moderator	0.684
Annular coolant channel	0.7605
Zircaloy cladding	0.786
Insulator	0.9

Materials definition

The composition of the most relevant materials, namely fuel and Zircaloy cladding, is reported in this sub-section.

```
% --- (U,Zr)C Fuel zone 1, 17% enrichment

mat fuel1_t1 -3.655

92238.09c  -1.4541E-1
92235.09c  -2.9784E-2
40090.09c  -4.8923E-1
 6000.09c  -3.3070E-1


% --- (U,Zr)C Fuel zone 2, 20% enrichment

mat fuel2_t1 -3.655
92238.09c  -1.4015E-1
92235.09c  -3.5044E-2
40090.09c  -4.8923E-1
 6000.09c  -3.3070E-1
```

```
% --- CERMET UO2 - ThO2 – W, fuel zone 1, 17 % enrichment

mat CERMET1_t1 -14.276
92238.09c  -3.14247E-1
92235.09c  -6.43667E-2
90232.09c  -2.60927E-2
 8016.09c  -5.45320E-2
74184.09c  -5.13729E-1
74183.09c  -2.70383E-2


% --- CERMET UO2 - ThO2 – W, fuel zone 2, 20 % enrichment

mat CERMET2_t1 -14.276
92238.09c  -3.02885E-1
92235.09c  -7.57214E-2
90232.09c  -2.60927E-2
 8016.09c  -5.45320E-2
74184.09c  -5.13729E-1
74183.09c  -2.70383E-2

% --- Cladding material Zircaloy-4

mat Zircaloy4_outer -6.56
 8016.06c  -1.19276E-03
24050.06c  -4.16117E-05
24052.06c  -8.34483E-04
24053.06c  -9.64457E-05
24054.06c  -2.44600E-05
26054.06c  -1.12572E-04
26056.06c  -1.83252E-03
26057.06c  -4.30778E-05
26058.06c  -5.83334E-06
40090.06c  -4.97862E-01
40091.06c  -1.09780E-01
40092.06c  -1.69646E-01
40094.06c  -1.75665E-01
40096.06c  -2.89038E-02
50112.06c  -1.27604E-04
50114.06c  -8.83732E-05
50115.06c  -4.59255E-05
50116.06c  -1.98105E-03
50117.06c  -1.05543E-03
50118.06c  -3.35688E-03
50119.06c  -1.20069E-03
50120.06c  -4.59220E-03
50122.06c  -6.63497E-04
50124.06c  -8.43355E-04
```

Pseudocode of the optimization step

The pseudocode to update the range in which the routine selects the input parameters is reported. It consists in a series of hierarchical constraints which gradually removes poor inputs values, leaving only the most promising for the design space exploration.

```
Read output from Serpent
Compute hot channel factor for each simulation
Create a list of arrays containing input and output data for any simulation
      #input includes simulation label, enrichment, axial and radial reflector
      #thickness, number of enrichment zone. Output includes k_eff, reactor mass
      #and hot channel factor.
Create an empty list to store simulation with keff<=1
Create an empty list to store simulation with keff>1
Create a list containing the parameters that are modified by the simulation

# Operational constraint
for any simulation:
      if keff<=1:
            append that simulation to list with keff<=1
      else
            append that simulation to list with keff>1

for any parameter:
      for any value of that parameter:
            count occurrencies of that value in list with keff<=1
            count occurrencies of that value in list with keff>1
            if (occurriencies in list with keff<=1) > (5 * (1+occurencies in list
with keff>1)):
                  remove that value from available parameter values
                        #corresponds to the Update range function in the
                        #flowchart

# Mass constraint

Create a list with reactors with axial and radial reflector thickness = upper
possible value of axial and radial reflector thickness
      Compute average keff from reactors from that list
Create a list with reactors with axial and radial reflector thickness = (upper-
1) possible value of axial and radial reflector thickness
      Compute average keff from reactors from that list

if average keff from upper list < 1.02 * average keff from (upper-1) list:
       # below 2% excess reactivity increase the mass increase is not worth

      remove upper value from the possible values of axial and radial reflector
thickness
            #corresponds to the Update range function in the flowchart
            #remove simulations from list with keff>1

# Temperature constraint

Create an empty list to store simulation with Fhc>2.8 # start with 3.5 then
decrease
Create an empty list to store simulation with Fhc<=2.8

for any simulation in list with keff>1:
      if Fhc>3:
            append that simulation to list with Fhc>2.8
```

```
      else
            append that simulation to list with Fhc<=2.8

for any parameter:
      for any value of that parameter:
            count occurrencies of that value in list with Fhc>2.8
            count occurrencies of that value in list with Fhc<=2.8

            if (occurriencies in list with keff<=1) > (5 * (1+occurencies in list
with keff>1))
                  remove that value from available parameter values
                        #corresponds to the Update range function in the flowchart
```